Glutathione S-transferase π localizes in mitochondria and protects against oxidative stress

Shinji Goto [1], Miho Kawakatsu [1], Shin-ichi Izumi [2], Yoshishige Urata [1], Kan Kageyama [1], Yoshito Ihara [3], Takehiko Koji [4] and Takahito Kondo [1].

1 Department of Biochemistry and Molecular Biology in Disease, Atomic Bomb Disease Institute, Nagasaki University Graduate School of Biomedical Sciences.

2 Department of Developmental and Reconstructive Medicine, Division of Oral Cytology and Cell Biology, Nagasaki University Graduate School of Biomedical Sciences.

3 Department of Biochemistry, Wakayama Medical University.

4 Department of Histology and Cell Biology, Nagasaki University Graduate School of Biomedical Sciences.

Address correspondence to: Shinji Goto, Ph.D., Department of Biochemistry and Molecular Biology in Disease, Atomic Bomb Disease Institute, Nagasaki University Graduate School of Biomedical Sciences, Nagasaki 851-8523, Japan.

Tel: ++81-(95)-819-7099; FAX: ++81-(95)-819-7100; E-Mail; sgoto@nagasaki-u.ac.jp

Running title: mitochondrial localization of GSTπ.

Acknowledgements. This work was supported in part by a Grant-in-Aid for the global Centers of Excellence program from the Ministry of Education, Science, Sports, Culture and Technology of Japan, and a Grant from the Basic Cancer Research Foundation of Japan.

Glutathione S-transferase π localizes in mitochondria and protects against oxidative stress

ABSTRACT

Glutathione S-transferases (GSTs) are multifunctional enzymes involved in the protection of cellular components against anti-cancer drugs or peroxidative stress. Previously we found that GSTπ, an isoform of GSTs, is transported into the nucleus. In the present study, we found that GSTπ is present in mitochondria as well as in the cytosol and nucleus in mammalian cell lines. A construct comprising the 84 amino acid residues in the amino-terminal region of GSTπ and green fluorescent protein was detected in the mitochondria. The mutation of arginine to alanine at positions 12,14,19,71, and 75 in full-length GSTπ completely abrogated the ability to distribute in the mitochondria, suggesting that arginine, a positively charged residue, is required for the mitochondrial transport of GSTπ. Chemicals generating reactive oxygen species such as rotenone and antimycin A decreased cell viability and reduced mitochondrial membrane potential. The overexpression of GSTπ diminished these changes. GSTπ-targeting siRNA abolished the protective effect of GSTπ on the mitochondria under oxidative stress. The findings indicate that the peptide signal is conductive to the mitochondrial localization of GSTπ under steady-state conditions without alternative splicing or post-translational modifications such as proteolysis, suggesting that GSTπ protects mitochondria against oxidative stress.

Key words- glutathione *S*-transferase π, mitochondria, mitochondrial targeting signal, rotenone, antimycin A,

oxidative stress

INTRODUCTION

Multiple enzymes exist in subcellular organelles to protect macromolecules such as nucleic acids, proteins, and lipids against chemicals and oxidative stress. Mitochondria are a center of energy metabolism utilizing oxygen, where reactive oxygen species (ROS) are produced under physiological conditions, and play a central role in regulating apoptosis (1-8). Mn-superoxide dismutase (SOD) is present in the mitochondrial matrix (1), Cu, Zn-SOD, a largely cytosolic enzyme, is located in the intermembrane space (IMS) of mitochondria (2), phospholipid hydroperoxide glutathione peroxidase (PHGPx, GPx4) is expressed as different isoforms in the nucleus, nucleoli, cytosol, and mitochondria (3, 4), classical glutathione peroxidase and glutathione reductase (GR) are found in both the cytosol and mitochondria (5, 6), two isoforms of glutaredoxins (Grx) are present in the cytosol, mitochondria, and nucleus (7), and thioredoxin (Trx) is expressed in the cytosol and mitochondria (8). These enzymes are thought to be important in maintaining physiological functions in each organelle.

Glutathione S-transferase (GST, EC 2.5.1.18) is a multifunctional enzyme involved in cellular detoxification (9, 10). Human GSTπ is part of a family of GSTs, and its expression increases in various

human cancer tissues, precancerous tissues (11-13), and cancer cell lines with acquired resistance to anti-cancer drugs (14-16). Previously, we demonstrated that inhibition of the nuclear accumulation of GSTπ increased anti-cancer drug- and hydrogen peroxide-induced DNA damage in cancer cell lines (17, 18).

GST isoforms in hepatic mitochondria have been reported in rats (19-21), mice (22-24), and humans (25, 26). However, the mitochondrial targeting signal (MTS) and the intra-mitochondrial localization of human GSTP1 have not been characterized. The majority of mitochondrial proteins are synthesized in the cytoplasm and subsequently transported into the mitochondria. Mitochondrial import proteins can be divided into two main classes (27-29). The first class comprises proteins that are destined for the mitochondrial matrix, as well as a number of proteins of the inner membrane and IMS, which carry N-terminal cleavable extensions with a MTS. The second class includes all outer membrane proteins, many IMS proteins, and inner membrane proteins with various internal MTSs. These precursors are synthesized without cleavable extensions (30, 31). Mn-SOD, the mitochondrial form of PHGPx, GR, and Trx2 are synthesized as precursor proteins containing a cleavable MTS in the N-terminal region in the cytoplasm and transported into the mitochondria (1, 4, 6, 8). Mitochondrial Grx2 has an internal MTS in the N-terminal region (7).

Cardiolipin (CL) is a unique phospholipid and located exclusively in the inner mitochondrial membrane.

Since CL is mainly comprised of polyunsaturated fatty acids, and the mitochondrial respiratory chain is a major source of ROS, CL is thought to be susceptible to peroxidation. CL plays a very important role in not only the anchoring of cytochrome *c* (cyt. *c*) to the mitochondrial inner membrane but also the optimal functioning of numerous enzymes involved in the mitochondrial respiratory chain and metabolism. Hence, alterations to the CL profile such as a decrease in content, peroxidation, and changes in composition may result in mitochondrial dysfunction (32). Peroxidation of CL results in the dissociation of cyt. *c* from mitochondrial inner membranes. It was reported that overexpression of mitochondrial PHGPx suppresses the generation of cardiolipin hydroperoxide (CL-OOH) and the release of cyt. *c* from mitochondrial inner membranes of 2-deoxyglucose-treated cells (33).

In the present study, we found that GSTπ is located not only in the cytosol and nucleus but also in the mitochondria in mammalian cell lines. We also identified the MTS of GSTπ. GSTπ has an internal MTS located at its N-terminal, a region not involved in the nuclear localization of GSTπ. The overexpression of GSTπ diminished the decrease in cell viability and loss of mitochondrial membrane potential induced by ROS–generating chemicals such as rotenone and antimycin A. GSTπ-targeting siRNA abolished the protective effect of GSTπ on the mitochondria under oxidative stress. The findings indicated that the peptide signal is conductive to the distribution of GSTπ in the mitochondria under steady-state conditions without

alternative splicing or post-translational modifications such as proteolysis, suggesting that GSTπ protects mitochondria against oxidative stress.

Materials and Methods

Materials- This section is described in detail in the supplemental section available online.

Preparation of GSTπ antibody- GSTπ was purified from human placenta as described by Satoh *et al*. (11), and a polyclonal antibody against human GSTπ was obtained by immunization of rabbits with the purified GSTπ as described by Shiratori *et al* (34).

Cell culture- See the supplemental section online.

Construction of vectors for protein expression- See the supplemental section online.

Generation of mutants- See the supplemental section online.

Preparation of cytosolic and nuclear proteins- The cytosolic and nuclear proteins were prepared as described

previously (17). Briefly, cell pellets ($1x10^6$ cells) were treated with 100 μl of hypotonic buffer (10 mM HEPES at pH 7.8, 10 mM KCl, 0.1 mM EDTA, 1 mM dithiothreitol, 0.5 mM phenylmethylsulfonylfluoride [PMSF], 2 μg/ml pepstatin, and 2 μg/ml leupeptin). After centrifugation of the sample (1,800 x *g*, 4°C, 1 min), the supernatant and debris were collected as rough cytosolic and nuclear fractions, respectively. The rough cytosolic fractions were centrifuged at 15,000 x *g* for 20min and 100,000 x *g* for 30min at 4°C. The final supernatant was collected as the cytosolic fraction. The rough nuclear fractions were washed three times with the hypotonic buffer and treated with 100 μl of 50 mM HEPES (pH 7.8), 420 mM KCl, 0.1 mM EDTA, 1 mM dithiothreitol, 5 mM $MgCl_2$, 0.5 mM PMSF, 2 μg/ml pepstatin, and 2 μg/ml leupeptin, and then gently rotated with a rotator at 4°C for 30 min. The supernatant was prepared as the nuclear fraction.

Isolation of mitochondria- Mitochondria were prepared as described by Matsuda *et al.* (35) and Vance (36) with a slight modification. Briefly, $1x10^8$ cells were washed twice with PBS and the cell pellet was suspended in 11 ml of hypotonic buffer [10 mM Tris-HCl (pH 7.5), 10 mM NaCl and 1.5 mM $MgCl_2$]. The cells were lysed by 10 strokes in a tight fitting Teflon glass homogenizer. Then 8 ml of 2.5 x MS buffer [12.5 mM Tris-HCl (pH 7.5), 25 mM mannitol, 175 mM sucrose, and 2.5 mM EDTA] was added to homogenates. The homogenates were centrifuged three times at 900 x *g* for 5 min at 4°C to remove nuclei

and debris. The supernatants were centrifuged at 5,000 x *g* for 10 min at 4°C to collect a crude mitochondrial fraction. The pellets were suspended in 500 μl of MS buffer, and then the suspension was subjected to discontinuous Percoll gradient (6%, 12%, 24%, 40% in MS buffer) centrifugation at 55,000 x *g* for 15 min at 4 °C. The material located at the interface of the lowest layers was collected and diluted 1:9 with MS buffer. To remove the Percoll, the samples were centrifuged at 10,000 x *g* for 10min at 4 °C and the pellet was washed twice with ice-cold MS buffer to obtain pure mitochondria.

Immunoblotting- Immunological levels of GSTπ, RCC1, Cu, Zn-SOD, AIF, Mn-SOD, GFP, cathepsin D, catalase, calnexin, and FLAG- or *myc*-tagged proteins in the cells were estimated by immunoblotting. Lysate (30 μg of total protein) from the extract of cells was separated by sodium dodecyl sulfate-polyacrylamide gel electrophoresis (SDS-PAGE) using a 12.5% or 15% gel, transferred to a nitrocellulose membrane, and immunologically stained with each appropriate primary antibody, and then with HRP-labeled anti-rabbit, anti-mouse, or anti-goat IgG as the secondary antibody. Blots were developed by enhanced chemiluminescence using the ECL kit. The protein concentration was determined according to Redinbaugh and Turley (37), with bovine serum albumin as the standard.

Immunohistochemistry- To identify the intracellular localization of endogenous GSTπ, cells were maintained with RPMI 1640 medium or DMEM containing 10% FBS on glass coverslips in a 6-well multi plate (Nalge Nunc International, Naperville, IL). Cells on the coverslips were washed three times with phosphate-buffered saline (PBS) and immersed in ice-cold 20 mM HEPES (pH7.3), 110 mM potassium acetate, 5 mM sodium acetate, 2 mM magnesium acetate, 1 mM EGTA, 2 mM DTT containing 30 μg/ml~40 μg/ml of digitonin, and 2 μg/ml each of aprotinin, leupeptin, and pepstatin. The cells were allowed to permeabilize for 3~4 min after which the digitonin-containing buffer was removed. Cells were fixed with 3% paraformaldehyde in PBS for 20 min, then rewashed three times with PBS and treated with 1% Triton-X 100 in PBS for 10 min. After three more washes with PBS and blocking with 3% bovine serum albumin in PBS for 1 h at room temperature, they were treated with anti-GSTπ antibody for 1h. After further washing with PBS, they were treated with FITC-conjugated anti-rabbit IgG for 30 min avoiding exposure to light. After another three washes with PBS, they were treated with anti-AIF antibody for 1h, then rewashed three times with PBS and treated with rhodamine-conjugated anti-mouse IgG for 30 min. They were washed with PBS and mounted in glycerol/PBS containing anti-fade reagent. Fluorescence intensity was observed under a confocal laser scanning microscope (LSM5 pascal, Carl Zeiss, Jena, Germany).

Evaluation of intracellular distribution of GFP-fused Proteins- The expression vectors (2 μg) for various GFP-fused proteins were transfected into COS-1 cells or HCT8 cells grown on glass coverslips with Lipofectamine reagent or Lipofectamine 2000. The fused proteins were expressed by cultivating the transfectants for 24 h at 37°C, and then fixed with 3% paraformaldehyde in PBS for 20 min. After three washes with PBS, the intracellular distribution of GFP-fused proteins was observed under a confocal laser scanning microscope. The location of the mitochondria was determined by staining the cells with MitoRed.

Immunoelectron microscopy- HCT8 cells were cultured in the wells of Lab Tek 4-well chamber slides (Nalge Nunc International, IL) for immunoelectron microscopy (38). The cells were washed with 0.01 M PBS, and fixed with a mixture of 4% paraformaldehyde and 0.1% glutaraldehyde in PBS for 15 min. The fixed cells were washed with PBS and embedded in LR-White resin. The resin was polymerized at 55 °C for 3 days and then ultrathin sections were mounted on nickel grids. They were reacted with rabbit anti-GSTπ IgG, followed by colloidal gold (15 nm)-labeled goat anti-rabbit IgG (British Biocell International, Cardiff, UK). After post-fixation with 1% glutaraldehyde in PBS, the sections were viewed in the transmission electron image mode with an accelerating voltage of 60 kV under a transmission electron microscope (JEOL 1200EX, JEOL Ltd., Tokyo, Japan). For the negative staining control, the sections were reacted with normal rabbit IgG

instead of the rabbit-anti-GSTπ IgG. To confirm the immunoreactivity of the mitochondrial antigens, the sections were reacted with mouse anti-mitochondria IgG (Leinco Technologies, Inc., St. Louis, MO) instead of the rabbit-anti-GSTπ IgG, followed by colloidal gold (10 nm)-labeled goat anti-mouse IgG (British Biocell International) for the positive staining control. For the negative staining control of the mitochondrial marker antigen, the tissues were reacted with normal mouse IgG instead of the mouse anti-mitochondria IgG.

Establishment of GSTπ gene-overexpressing HCT8 cells The introduction of pcDNA3/FLAG-HA-GSTπ1-210 into HCT8 was performed by a lipofection method using Lipofectamine 2000. HCT8 cells transfected with an expression vector not containing the insert of GSTπ cDNA (mock) were used as a control. Stable transfectants were obtained by a step-wise addition of G418 to the culture medium at 150 μg/ml to 500 μg/ml over a one-month period. The cloned G418-resistant lines were screened for the expression of GSTπ. FLAG-HA-GSTπ1-210-expressing-clonal cell lines (FHGC-16) and a mock-transfected cell line (VecC-12) were obtained.

siRNA silencing of GSTπ expression-GSTπ expression was silenced using a pre-designed GSTπ-targeting siRNA. The GSTπ-targeting or negative control siRNA was introduced into HCT8 cells using lipofectamine

2000. Cells were incubated for an additional 48 h, and then used to analyze GSTπ expression and in further experiments.

GST activity assay - Total GST activity was determined by measuring the rate of conjugation of 1-chloro-2, 4-dinitrobenzene (CDNB) with reduced glutathione as described previously (17). Briefly, GST activity was measured in the presence of 1 mM GSH and 1 mM CDNB in 0.1 M sodium phosphate buffer (pH 6.5). The DNP-GSH conjugate was detected at 340 nm and the rate of increase in absorbance is directly proportional to the GST activity in the sample.

Cell viability- Cell viability was estimated by the MTT assay as described (39). Briefly, cells (5000) were placed in 100 μl of medium per well in 96-well plates. At twenty four hours of treatment with various concentrations of rotenone, antimycin A, or potassium cyanide, the cells were incubated for 4 h at 37 °C with 3-(4,5-dimethylthiazol-e-yl)-2,5-diphenyltetrazolium bromide (652 μg/ml) and lysed with 100 μl of 20% SDS, 50% N, N-dimethylformamide (pH 4.7) in each well. After an overnight incubation at 37 °C, the absorbance at 570 nm was measured. Wells without cells served as blanks. Cell viability was also estimated by measuring of the activity of LDH remaining after treatment with inhibitors of the mitochondrial respiratory

chain using a MTX-LDH kit. Cells (5000) were placed in 100 μl of medium per well in 96-well plates. After 24 h of treatment, the medium was removed, and the wells were washed with PBS twice. LDH activity was estimated according to the manufacturer's instructions. Wells without cells served as blanks.

Flow cytometric analyses- The detection of mitochondrial superoxide in living cells was performed by using a MitoSOX Red mitochondrial superoxide indicator. Briefly, approximately 2 x 10^6 cells were harvested, and suspended in culture medium containing 5 μM MitoSOX Red at 37 °C for 10-20 min. To assess mitochondrial membrane potential, the harvested cells were suspended in culture medium containing 10 μM rhodamine 123 for 15min at 37 °C. After the washing out of the fluorescent dye, the cells were resuspended in PBS, and fluorescence intensity was estimated using a FACScan flow cytometer (Becton Dickinson, San Jose, CA).

Statistical analysis-Data are presented as mean ± S.D. Differences were examined using Student's t test. A value of $P < 0.05$ was considered significant.

Results

Intracellular localization of endogenous GSTπ- The intracellular localization of endogenous GSTπ was evaluated by immunoblotting using HCT8, A549, and COS-1 cells (**Fig. 1A**). Compared to RCC1, a marker of nuclear protein, AIF, a marker of mitochondrial protein, and Cu, Zn-SOD, a marker of cytosolic protein, GSTπ was found in each fraction under steady-state conditions with a similar molecular size. The purity of prepared mitochondrial fractions was evaluated in detail by immunoblot analysis using antibodies against calnexin, a marker of the endoplasmic reticulum, catalase, a marker of peroxisomes, and cathepsin D, a marker of lysosomes. (**Fig. 1B**). These proteins were not detected in the prepared mitochondrial fractions. In addition, the intracellular distribution of endogenous GSTπ was analyzed by immunohistochemistry using anti-GSTπ and anti-AIF antibodies (**Fig. 1C**). The cytosol of cells was rich in endogenous GSTπ (**Fig. 1A**). This is a major problem since the extensive cytosolic staining precludes demonstrating the mitochondrial localization of GSTπ by immunohistochemistry. To address this issue, cells were treated with digitonin to permeabilize the plasma membrane for depletion of the cytosolic pool of GSTπ prior to fixation. The co-localization of GSTπ with AIF in the mitochondria of HCT8, A549, and COS-1 cells was observed under

steady-state conditions (**Fig. 1C**). These results suggest that endogenous GSTπ is also expressed in the mitochondria of the mammalian cell lines.

GSTπ is expressed inside mitochondria- To know the intra-mitochondrial distribution of GSTπ, we performed an immunoelectron microscopic analysis. Immunoelectron microscopic micrographs of HCT8 cells are presented in Figure 1D. The sections were immunoreacted with rabbit anti-GSTπ IgG, followed by colloidal gold-labeled goat anti-rabbit IgG. As shown in Figure 1D**(**a**)**, colloidal gold particles were seen on the inner membrane (short arrow) and cristae membrane (long arrow) of the mitochondria. The sections were immunoreacted with mouse anti-mitochondria IgG, followed by colloidal gold-labeled goat anti-mouse IgG, and smaller colloidal gold particles were seen in the mitochondria (short and long arrows) (**Fig. 1D**(**c**)). Alternatively, the sections were immunoreacted with normal rabbit IgG followed by colloidal gold-labeled goat anti-rabbit IgG (**b**) or immunoreacted with normal mouse IgG followed by colloidal gold-labeled goat anti-mouse IgG (**d**), and no colloidal gold particles were seen in the mitochondria. Additionally, to confirm the intra-mitochondrial distribution of GSTπ, intact mitochondrial fractions were treated with pronase (0-50 μg/ml) for 30min on ice and subjected to immunoblot analysis. Bcl-2, a mitochondrial outer membrane protein, was completely degraded by pronase (20 μg/ml), whereas GSTπ remained in the mitochondrial

fractions on treatment with pronase (50 μg/ml) as well as AIF, which is located inside the mitochondria (data not shown). These results suggest that GSTπ is present inside the mitochondria.

GSTπ has an internal MTS- Some proteins in mitochondria have internal targeting signals at the N-terminal, which are not cleaved (27-29). Then, we examined if GSTπ has an uncleaved internal targeting signal. pcDNA3/FLAG-GSTπ1-210 was transiently transfected into COS-1 cells, and the expression of FLAG-GSTπ1-210 was examined by immunoblot analysis using anti-FLAG and anti-GSTπ antibodies (**Fig. 2A**). The molecular size of FLAG-GSTπ1-210 in the extract from the cytosol and mitochondria was similar, suggesting that GSTπ has an internal MTS.

We were interested in the N-terminal region for identification of the MTS of GSTπ. We constructed expression vectors encoding different N-terminal regions of GSTπ fused to the N-terminal end of GFP (**Fig. 2B**), and introduced these vectors in COS-1 cells. All of the various GSTπ-GFPs were expressed with the same apparent molecular size as GFP-fused proteins (data not shown). Subsequently, the intracellular localization of GSTπ-GFPs was observed under a confocal laser scanning microscope. As shown in Figure 2C and supplemental Figure 1, GFP alone, GSTπ1-44-GFP, GSTπ1-60-GFP, and GSTπ1-70-GFP expressed in COS-1 cells were not detected in mitochondria. Only GSTπ1-84-GFP was exclusively localized to

mitochondria without cytoplasmic and nuclear accumulation. Interestingly, GSTπ20-84-GFP, deleted of amino acids 1-19 from the 1-84 region, showed no mitochondrial accumulation. From these results, the 1-84 amino acid region, especially regions 1-19 and 71-84, may be required for the mitochondrial transport of GSTπ.

To further define the MTS of GSTπ, a point mutation from arginine to alanine was generated by site-directed mutagenesis with pcDNA3.1/ GSTπ1-84-GFP as the template. GSTπ1-84(R12A)-GFP, GSTπ1-84(R14A)-GFP, GSTπ1-84(R19A)-GFP, GSTπ1-84(R71A)-GFP, and GSTπ1-84(R75A)-GFP were partially co-localized with MitoRed in COS-1 cells (**supplemental Fig. 2)**. On the other hand, a series of double mutants such as GSTπ1-84(R12,14A)-GFP, GSTπ1-84(R12,19A)-GFP, GSTπ1-84(R14,19A)-GFP, and GSTπ1-84(R71,75A)-GFP completely lost the ability to accumulate in the mitochondria (**Fig. 2D**). These findings indicate that region 1-84 of GSTπ has potential as a MTS, however, they also raised the question of whether the distribution of truncated forms of GSTπ has physiological relevance. It is well known that proteins often contain cryptic targeting signals that are not functionally important. To demonstrate the actual function of the MTS identified in the full-length GSTπ, we constructed expression vectors encoding a myc-tagged full-length GSTπ (pcDNA3.1/GSTπ1-210-myc) and the mutation of arginine to alanine at positions 12,14,19,71, and 75 in myc-tagged full-length GSTπ (pcDNA3.1/GSTπ1-210-myc mutant). These

vectors were introduced into COS-1 cells, and the mitochondrial distribution of myc-tagged wild-type and mutant GSTπ was evaluated by immunoblot analysis using anti-GSTπ and anti-myc antibodies in the prepared mitochondrial fraction. It was observed that myc-tagged wild-type GSTπ was expressed in the mitochondria with endogenous GSTπ, whereas mutant GSTπ completely lost the ability to accumulate in the mitochondria (**Fig. 2E**). These results suggest that arginine, a positively charged residue, in the MTS is required for the mitochondrial transport of GSTπ.

Establishment of GSTπ gene-overexpressing HCT8 cells-To investigate the role of GSTπ in the mitochondria under oxidative stress, we established a FLAG-HA-tagged full-length GSTπ-expressing clonal cell line (FHGC-16). A mock-transfected cell line (VecC-12) was employed as a control. As shown in Figure 3A upper panel, FLAG-HA-GSTπ1-210 was present in lysate of the cytosol, the nucleus, and mitochondria from FHGC-16 cells. In Figure 3A lower panel, GST activity was greater in lysate of the cytosol, the nucleus, and mitochondria in FHGC-16 cells than VecC-12 cells.

The overexpression of GSTπ diminishes the cytotoxicity of inhibitors for the mitochondrial respiratory chain-To evaluate the effect of overexpressed GSTπ on the cytotoxicity of inhibitors for the mitochondrial

respiratory chain, FHGC-16 cells and VecC-12 cells were treated with various concentrations of rotenone (inhibitor for complex I), antimycin A (inhibitor for complex III), or potassium cyanide (inhibitor for complex IV) for 24 h, and cell viability was estimated by the MTT assay (**Fig. 3B**) and LDH assay (**supplemental Fig. 3)**. The cytotoxicity of rotenone or antimycin A was markedly decreased in FHGC-16 cells compared with VecC-12 cells. On the other hand, no significant cytotoxic effect was observed with potassium cyanide. The results indicate that the overexpression of GSTπ diminishes the cytotoxicity of rotenone or antimycin A in HCT8 cells. To examine the role of superoxide in the cytotoxicity, production of mitochondrial superoxide was estimated flow-cytometrically using a MitoSOX Red mitochondrial superoxide indicator. As shown in Figure 3C, the fluorescence intensity derived from the generation of superoxides increased in FHGC-16 cells and VecC-12 cells treated with 350 μM rotenone or 150 μM antimycin A for 1h and levels remained high for up to 6 h in both lines. Whereas, no increase in fluorescence intensity was observed in the cells treated with 5 mM potassium cyanide. These results suggest a close relationship between the cytotoxicity of rotenone or antimycin A and the production of superoxides in mitochondria. There was no detectable difference in superoxide production between the resistant cells (FHGC-16) and sensitive cells (VecC-12). The difference in sensitivity to rotenone or antimycin A may be due to the enhanced antioxidative capacity of FHGC-16 cells.

The overexpression of GSTπ prevents the loss of mitochondrial membrane potential- To further evaluate the effect of GSTπ overexpression on the mitochondrial dysfunction induced by antimycin A, the alteration of mitochondrial membrane potential was examined by flow cytometry using rhodamine 123 as a fluorescent probe. The fluorescence intensity reflecting mitochondrial membrane potential decreased in VecC-12 cells treated with 150 μM antimycin A for 6 h, and further decreased up to 24 h (**Fig. 3D**). In contrast, the fluorescence intensity in FHGC-16 cells treated with 150 μM antimycin A for 24 h was significantly higher than in VecC-12 cells. These results suggest that the overexpression of GSTπ plays a role in the retention of mitochondrial membrane potential.

GSTπ-targeting siRNA enhances cytotoxicity and loss of mitochondrial membrane potential –To further confirm its role, GSTπ was silenced using a pre-designed GSTπ-targeting siRNA. The GSTπ-targeting or negative control siRNA was introduced into FHGC-16 and VecC-12 cells. These cells were incubated for 48 h, and the expression of GSTπ was analyzed by immunoblotting (**Fig. 4A upper panel**). The expression of endogenous GSTπ and FLAG-HA-GSTπ$_{1\text{-}210}$ was diminished in the isolated mitochondrial fraction prepared from the cells transfected with GSTπ-targeting siRNA compared with that of cells transfected with negative control siRNA. GST activity markedly deceased in lysates of isolated mitochondria from FHGC-16 and

VecC-12 cells transfected with GSTπ-targeting siRNA compared with FHGC-16 and VecC-12 cells transfected with negative control siRNA (**Fig. 4A lower panel**). To evaluate the effect of diminished GSTπ expression on mitochondrial dysfunction, mitochondrial membrane potential was examined by flow cytometry in the presence or absence of antimycin A. The level of fluorescence was reduced in VecC-12 cells transfected with GSTπ-targeting siRNA, when these cells were treated with antimycin A for specified periods (**Fig. 4B**). Next, the effect of diminished GSTπ expression on cell viability was examined by the MTT assay and LDH assay. As shown in figure 4C and supplemental figure 4, the cytotoxicity of antimycin A increased in GSTπ-siRNA transfectants compared with the control. These findings indicate that GSTπ-targeting siRNA enhances antimycin A-induced loss of mitochondrial membrane potential and cytotoxicity.

Discussion

In the present study, we found evidence for the first time that

1) Endogenous GSTπ exists in the mitochondria of mammalian cell lines with a similar molecular size to the cytosolic form.

2) Eighty four amino acid residues in the N-terminal region of GSTπ, especially the positively charged

residues at 1-19 and 71-84, were required for the localization in mitochondria.

3) The overexpression of GSTπ diminishes the cytotoxicity and loss of mitochondrial membrane potential induced by rotenone or antimycin A.

Localization of GSTπ in mitochondria depends on peptide signals – There have been studies on the nuclear and mitochondrial distribution of proteins. For example, Abasic-endonuclease 1(APE1), a key enzyme of DNA base excision repair, occurs in both the nucleus and mitochondria. The nuclear APE1 is intact, whereas the mitochondrial APE1 lacks 33 N-terminal amino acid residues including the nuclear localization signal (NLS), suggesting that cleavage of APE1 by a specific mitochondria-associated N-terminal peptidase is a prerequisite for the mitochondrial import of APE1 (41). Chloride intracellular channel protein (CLIC4/mtCLIC) distributes to the mitochondria and cytoplasm of keratinocytes under physiological conditions. Suh *et al.* showed that apoptotic/stress-inducing agents cause an association of CLIC4 with Ran, NTF2, and Importin-α, and then allow the cytoplasmic CLIC4 to enter the nucleus (42). The human *TOP3α* gene encoding DNA topoisomerase IIIα (hTop3α) has two potential start codons for the synthesis of proteins 1,001 and 976 amino acid residues in length. HTop3α is located in both the nucleus and mitochondria, the former having a mitochondrial form (43). PHGPx is encoded by a single gene, *gpx-4*, that has two distinct promoter regions. The upstream region transcribes cytosolic PHGPx and mitochondrial PHGPx, while the

downstream region yields nuclear PHGPx (3). Human Grx2 is synthesized in both nuclear and mitochondrial forms from a single gene by differential splicing. Mitochondrial Grx2 has an internal MTS in the N-terminal region, but the precise NLS of nuclear Grx2 has not been determined (7).

We found that endogenous mitochondrial GSTπ was of a similar molecular size to cytosolic GSTπ under steady-state conditions (**Fig. 1**). FLAG-tagged GSTπ1-210 and myc-tagged GSTπ1-210 were also located in the mitochondria (**Figs. 2A and E**). We purified GSTπ from human placenta and prepared a GSTπ antibody as described in the Materials and Methods. We previously indicated that there was a difference in the recognition of GST protein between our GSTπ antibody and antibodies against human GSTA1-1 or GSTM1-1 (39). Additionally, our antibody recognized exogenous FLAG-tagged and myc-tagged GSTπ in the present study (Fig.2A, E and 3A). For these reasons, we conclude that the antibody does not recognize other isoforms of GST. This finding indicates that the distribution of GSTπ in the mitochondria depends on the internal peptide signals without alternative splicing or post-translational modifications such as proteolysis.

The MTS of GSTπ- Robin *et al.* have investigated the mechanism by which recombinant mouse GSTA4-4 is recruited to mitochondria using *in vivo* and *in vitro* systems. They showed that the MTS of GSTA4-4 was located at the C-terminal end (44). In contrast, we found that amino acid residues 1-84 at the N-terminal made up the MTS of GSTπ (**Fig. 2**). It was found that the MTS of GSTπ has no sequence similarity to

proteins except for the same subclass of GST found in other species by an analysis using the BLAST Network Service of UniProt Knowledgebase Release 8.0, developed by the Swiss-Prot group at the Swiss Institute of Bioinformatics and at the European Bioinformatics Institute. Moreover, we also confirmed that registered motifs were not found in the MTS of GSTπ in PROSITE, a database of protein families and domains prepared by the Swiss-Prot group and ISREC bioinformatics group of the Swiss Institute of Bioinformatics. Mitochondrial proteins have individual targeting signals, and some proteins lack a cleavable N-terminal presequence (27-29). The results obtained in the present study indicate that GSTπ has an uncleavable MTS.

In general, the majority of mitochondrial matrix proteins have presequences consisting of 15–40 amino acid residues. The presequence is rich in positively charged and hydroxylated amino acid residues which form an amphipathic helix. The formation of an amphipathic helix is believed to be essential for the import of proteins from the cytosol to the mitochondrial matrix (45). It is known that cytosolic chaperones such as Hsp70 interact with newly synthesized proteins and play a role in their import into mitochondria (44, 46). Furthermore, the amphipathic helix can interact with mitochondrial import receptors or susceptibility factors (27-29). Robin *et al*. showed that the Hsp70 chaperone is required for the efficient translocation of GSTA4-4 to mitochondria (44). The possible interaction of the MTS of GSTπ with chaperones or receptors cannot be ruled out. As for GSTπ, positively charged residues in the MTS were necessary for its import into the

mitochondria (**Fig. 2D**). However, a helical wheel analysis revealed that the MTS of GSTπ forms only an incomplete amphipathic helix (data not shown). One possible explanation is that the distribution of GSTπ in the intermembrane space or on the inner membrane of mitochondria is caused by an incomplete amphipathic helix (**Fig. 1D**). At present, the mechanisms for the targeting and uptake of intermembrane space proteins are not well understood compared with those for proteins of other mitochondrial compartments. Further study of the mechanisms for transport of the mitochondrial GSTπ is necessary.

4) *The role of GSTπ located in mitochondria*- When cancer cells were treated with anti-cancer drugs, the amount of GSTπ increased in the nucleus (17) as well as in the mitochondria (data not shown). These findings suggest that GSTπ in the subcellular organelles is involved in the acquisition of resistance of cancer cells to anti-cancer drugs. We found evidence that GSTπ is distributed in mitochondria via the internal MTS (**Figs. 2A and E**). At the present time, however, the regulatory mechanism of the distribution of GSTπ in mitochondria has not been clarified, and we could not control the abundance of GSTπ in the mitochondria. Hence, we investigated the role of the mitochondrial GSTπ against oxidative stress using GSTπ–overexpressing cells. The introduction of the GSTπ gene into HCT8 cells caused an accumulation of GSTπ in mitochondria and diminished the cytotoxicity of rotenone or antimycin A (**Fig. 3**). On the other hand, GSTπ-targeting siRNA abolished the protective effect of GSTπ on the

mitochondria under oxidative stress in GSTπ–overexpressing (FHGC-16) cells (**Fig. 4**). Mitochondria play a central role in the control of apoptosis triggered by the release of cyt. *c*. Cyt. *c* binds mainly to CL, which is distributed on the mitochondrial inner membrane under physiological conditions. Since CL is particularly rich in polyunsaturated fatty acids, it is easily peroxidized and converted to CL-OOH. Nomura *et al.* reported that the generation of CL-OOH in mitochondria occurred before the release of cyt. *c* in cells that had been induced to undergo apoptosis (33). They also observed that the release of cyt. *c* was suppressed when the production of CL-OOH in mitochondria was inhibited by the overexpression of mitochondrial PHGPx. CL plays a very important role in not only the anchoring of cyt. *c* to the mitochondrial inner membrane but also the optimal functioning of numerous enzymes that are involved in the mitochondrial respiratory chain and metabolism. Alterations of the CL profile such as a decrease in content, peroxidation, and changes in composition may also result in mitochondrial dysfunction (32). Garry *et al.* reported that cultured lung fibroblasts isolated from adult mice heterozygous for a PHGPx null allele (GPx4+/- LFs) were significantly more susceptible to hydrogen peroxide, cadmium, and cumene hydroperoxide-induced cytotoxicity. They also found that GPx4+/- LFs have lower mitochondrial membrane potential, and greater CL oxidation than LFs isolated from wild-type mice (47). GST7-7, a rat GST isoform which corresponds to human GSTπ, also has GSH peroxidase activity towards a number of

substrates including linoleate hydroperoxides and arachidonate hydroperoxi des (9). Taken together, mitochondrial GSTπ may protect mitochondria from oxidative stress by preventing the formation of CL-OOH.

The generation of reactive aldehydes such as 4-hydroxy-2-nonenal (4-HNE) and 4-oxo-2-nonenal (4-ONE) is derived from peroxidation of membrane lipids. Raza *et al.* identified rat GSTA4-4 in the mitochondrial matrix (24). Gardner *et al.* previously characterized the expression of GSTA4-4 in human liver mitochondria (25). GSTA4-4 and the A4-4 subclass of GST found in other species function to form a conjugate of 4-HNE with GSH (48, 49). We previously reported that GSTπ catalyzed the formation of 4-ONE conjugated with GSH to detoxify reactive aldehyde (18). These findings also raise the possibility that GSTπ protects mitochondria under oxidative stress by catalyzing the formation of reactive aldehydes conjugated with GSH in the mitochondria and contributes to cell survival. However, it may be possible for GSTπ overexpressed in other parts of the cell (nucleus or cytosol) to alter cell signaling which can account for the mitochondrial protection.

The physiological role of the mitochondrial GSTπ could not be elucidated entirely. However, the data obtained in the present study strongly suggest that GSTπ protects mitochondria against oxidative stress. Elucidation of the physiological significance and the transport mechanism of mitochondrial GSTπ may

facilitate the establishment of more efficient anti-cancer therapy.

Acknowledgments

The authors are grateful to Mr. Takashi Suematsu (Electron Microscope Center, Nagasaki University School of Medicine) for expert technical assistance with the electron microscopic analysis.

Abbreviations: GSH, reduced form of glutathione; GST, glutathione S-transferase; MTS, mitochondrial targeting signal; GFP, green fluorescent protein; PCR, polymerase chain reaction; HRP, horseradish peroxidase; FITC, fluorescein isothiocyanate; siRNA, small interfering RNA; RCC1, regulator of chromosome condensation 1; AIF, apoptosis–inducing factor; Cu,Zn-SOD, Cu,Zn-superoxide dismutase; Mn-SOD, Mn-superoxide dismutase; GPx, glutathione peroxidase; CL, cardiolipin; cyt.*c*, cytochrome c; ROS, reactive oxygen species; 4-ONE, 4-oxo-2-nonenal; 4-HNE, 4-hydroxy-2-nonenal;

References

[1] Roise, D.; Schatz, G. Mitochondrial presequences. *J. Biol. Chem.* **263:** 4509-4511; 1988.

[2] Sturtz, L.A.; Diekert, K.; Jensen, R.; Lill, L.T.; Culotta, V.C. A fraction of yeast Cu,Zn-superoxide

dismutase and its metallochaperone, CCS, localize to the intermembrane space of mitochondria. A physiological role for SOD1 in guarding against mitochondrial oxidative damage. *J. Biol. Chem.* **276:** 38084-38089; 2001.

[3] Borchert, A.; Savaskan, N.E.; Kuhn, H. Regulation of expression of the phospholipid hydroperoxide/sperm nucleus glutathione peroxidase gene. Tissue-specific expression pattern and identification of functional cis- and trans-regulatory elements. *J. Biol. Chem.* **278:** 2571-2580; 2002.

[4] Arai, M.; Imai, H.; Sumi, D.; Imanaka, T.; Takano, T.; Chiba, N.; Nakagawa, Y. Import into mitochondria of phospholipid hydroperoxide glutathione peroxidase requires a leader sequence. *Biochem. Biophys. Res. Commun.* **227:** 433-439; 1996.

[5] Esworthy, R.S.; Ho, Y.S.; Chu, F.F. The Gpx1 gene encodes mitochondrial glutathione peroxidase in the mouse liver. *Arch. Biochem. Biophys.* **340:** 59-63; 1997.

[6] Outten, C.E.; Culotta, V.C. Alternative start sites in the Saccharomyces cerevisiae GLR1 gene are responsible for mitochondrial and cytosolic isoforms of glutathione reductase. *J. Biol. Chem.* **279:** 7785-7791; 2004.

[7] Lundberg, M.; Johansson, C.; Chandra, J.; Enoksson, M.; Jacobsson, G.; Ljung, J.; Johansson, M.; Holmgren, A. Cloning and expression of a novel human glutaredoxin (Grx2) with mitochondrial and nuclear

isoforms. *J. Biol. Chem.* **276:** 26269-26275; 2001.

[8] Spyrou, G.; Enmark, E.; Miranda-Vizuete, A.; Gustafsson, J. Cloning and expression of a novel mammalian thioredoxin. *J. Biol. Chem.* **272:** 2936-2941; 1997.

[9] Chasseaud, L.F. The role of glutathione and glutathione S-transferases in the metabolism of chemical carcinogens and other electrophilic agents. *Adv. Cancer Res.* **29:** 175-274; 1979.

[10] Meyer, D. J.; Beale, D.; Tan, K.H.; Coles, B.; Ketterer, B. Glutathione transferases in primary rat hepatomas: the isolation of a form with GSH peroxidase activity. *FEBS Lett.* **184:** 139-143; 1985.

[11] Satoh, K.; Kitahara, A.; Soma, Y.; Inaba, Y.; Hatayama, I.; Sato, K. Purification, induction, and distribution of placental glutathione transferase: a new marker enzyme for preneoplastic cells in the rat chemical hepatocarcinogenesis. *Proc. Natl. Acad. Sci. USA* **82:** 3964-3968; 1985.

[12] Mannervik, B.; Castro, V.M.; Danielson, U.H.; Tahir, M.K.; Hansson, J.; Ringborg, U. Expression of class Pi glutathione transferase in human malignant melanoma cells. *Carcinogenesis* **8:** 1929-1932; 1987.

[13] Howie, A.F.; Forrester, L.M.; Glancey, M.J.; Schlager, J.J.; Powis, G.; Beckett, G.J.; Hayes, J.D.; Wolf, C.R. Glutathione S-transferase and glutathione peroxidase expression in normal and tumour human tissues. *Carcinogenesis* **11:** 451-458; 1990.

[14] Saburi, Y.; Nakagawa, M.; Ono, M.; Sakai, M.; Muramatsu, M.; Kohno, K.; Kuwano, M. Increased

expression of glutathione S-transferase gene in cis-diamminedichloroplatinum(II)-resistant variants of a Chinese hamster ovary cell line. *Cancer Res.* **49:** 7020-7025; 1989.

[15] Batist, G.; Tulpule, A.; Sinha, B.K.; Katki, A.G.; Myers, C.E.; Cowan, K.H. Overexpression of a novel anionic glutathione transferase in multidrug-resistant human breast cancer cells. *J. Biol. Chem.* **261:** 15544-15549; 1986.

[16] Wang, Y.Y.; Teicher, B.A.; Shea, T.C.; Holden, S.A.; Rosbe, K.W.; al-Achi, A.; Henner, W. D. Cross-resistance and glutathione-S-transferase-pi levels among four human melanoma cell lines selected for alkylating agent resistance. *Cancer Res.* **49:** 6185-6192; 1989.

[17] Goto, S.; Ihara Y.; Urata, Y.; Izumi, S.; Abe, K.; Koji, T.; Kondo, T. Doxorubicin-induced DNA intercalation and scavenging by nuclear glutathione S-transferase π. *FASEB J.* **14:** 2702-2714; 2001.

[18] Kamada, K.; Goto, S.; Okunaga, T.; Ihara, Y.; Tsuji, K.; Kawai, Y.; Uchida, K.; Osawa, T.; Matsuo, T.; Nagata, I.; Kondo, T. Nuclear glutathione S-transferase π prevents apoptosis by reducing the oxidative stress-induced formation of exocyclic DNA products. *Free Radical. Biol. Med.* **37:** 1875-1884; 2004.

[19] Harris, J.M.; Meyer, D.J.; Coles, B.; Ketterer, B. A novel glutathione transferase (13-13) isolated from the matrix of rat liver mitochondria having structural similarity to class theta enzymes. *Biochem. J.* **278:** 137–141; 1991.

[20] Kraus, P.; Wigand, J.; Ostermaier, R. Mitochondrial glutathione transferases. The alkylation of mitochondrial membrane yields a catalyst with glutathione-transferase-like properties. *Biol. Chem. Hoppe. Seyler.* **367:** 937–941; 1986.

[21] Bhagwat, S.V.; Vijayasarathy, C.; Raza, H.; Mullick, J.; Avadhani, N.G. Preferential effects of nicotine and 4-(N-methyl-N-nitrosamine)-1-(3-pyridyl)-1-butanone on mitochondrial glutathione S-transferase A4-4 induction and increased oxidative stress in the rat brain. *Biochem. Pharmacol.* **56:** 831–839; 1998.

[22] Addya, S.; Mullick, J.; Fang, J.K.; Avadhani, N.G. Purification and characterization of a hepatic mitochondrial glutathione S-transferase exhibiting immunochemical relationship to the alpha-class of cytosolic isoenzymes. *Arch. Biochem. Biophys.* **310:** 82–88; 1994.

[23] Jowsey, I.R.; Thomson, R.E.; Orton, T.C.; Elcombe, C.R.; Hayes, J.D. Biochemical and genetic characterization of a murine class Kappa glutathione S-transferase. *Biochem. J.* **373:** 559–569; 2003.

[24] Raza, H.; Robin, M.A.; Fang, J.K.; Avadhani, N.G. Multiple isoforms of mitochondrial glutathione S-transferases and their differential induction under oxidative stress. *Biochem. J.* **366:** 45-55; 2002.

[25] Gardner, J.L.; Gallagher, E.P. Development of a peptide antibody specific to human glutathione S-transferase alpha 4-4 (hGSTA4-4) reveals preferential localization in human liver mitochondria. *Arch. Biochem. Biophys.* **390:** 19–27; 2001.

[26] Gallagher, E.P.; Gardner, J.L.; Barber, D.S. Several glutathione S-transferase isozymes that protect against oxidative injury are expressed in human liver mitochondria. *Biochem. Pharmacol.* **71:** 1619-1628; 2006.

[27] Rapaport, D. Biogenesis of the mitochondrial TOM complex. *Trends Biochem. Sci.* **27:** 191-197; 2002.

[28] Wiedemann, N.; Frazier, A.E.; Pfanner, N. The protein import machinery of mitochondria. *J. Biol. Chem.* **279:** 14473-14476; 2004.

[29] Koehler, C. New developments in mitochondrial assembly. Annu. *Rev. Cell Dev. Biol.* **20:** 309-335; 2004.

[30] Koehler, C.M.; Merchant, S.; Schatz, G. How membrane proteins travel across the mitochondrial intermembrane space. *Trends Biochem. Sci.* **24:** 428-432; 1999.

[31] Pfanner, N.; Geissler, A. Versatility of the mitochondrial protein import machinery. *Nat. Rev. Mol. Cell. Biol.* **2:** 339-349; 2001.

[32] Chicco, A.J,; Sparagna, G.C. Role of cardiolipin alterations in mitochondrial dysfunction and disease. *Am. J. Physiol. Cell. Physiol.* **292:** 33-44; 2007.

[33]Nomura, K.; Imai, H.; Koumura, T.; Kobayashi, T.; Nakagawa, Y. Mitochondrial phospholipid hydroperoxide glutathione peroxidase inhibits the release of cytochrome c from mitochondria by suppressing the peroxidation of cardiolipin in hypoglycaemia-induced apoptosis. *Biochem. J.* **351:** 183–193; 2000.

[34] Shiratori, Y.; Soma, Y.; Maruyama, H.; Sato, S.; Takano, A.; Sato, K. Immunohistochemical detection of the placental form of glutathione S-transferase in dysplastic and neoplastic human uterine cervix lesions. Cancer Res. **47:** 6806-6809; 1987.

[35] Matsuda, K.; Yoshida, K.; Taya, Y.; Nakamura, K.; Nakamura, Y.; Arakawa, H. p53AIP1 regulates the mitochondrial apoptotic pathway. *Cancer Res.* **62:** 2883-2889; 2002.

[36] J.E. Vance, Phospholipid synthesis in a membrane fraction associated with mitochondria, J. Biol. Chem. **265** 7248–7256 1990.

[37] Redinbaugh, M.G.; Turley, R.B. Adaptation of the bicinchoninic acid protein assay for use with microtiter plates and sucrose gradient fractions. *Anal. Biochem.* **153:** 267-271; 1986.

[38] Izumi, S.; Kimura, M.; Kimura, T.; Wada, A.; Hirayama, T.; Ichinose, A.; Koji, T. Induction of active invagination of plasma membranes by Helicobacter pylori cytotoxin, VacA, in cultured gastric cells: An immunoelectron microscopic study. *Acta Histochem. Cytochem.* **33:** 89-94; 2000.

[39] Goto, S.; Kamada, K.; Soh, Y.; Ihara, Y.; Kondo, T. Significance of nuclear glutathione S-transferase π in resistance to anti-cancer drugs. *Jpn. J. Cancer Res.* **9:** 1047–1056; 2002.

[40] Reipert, S.; Berry, J.; Hughes, M. F.; Hickman, J. A.; Allen, T. D. Changes of mitochondrial mass in the hemopoietic stem cell line FDCP-Mix after treatment with etoposide: a corelative study by multiparameter

flow cytometry and confocal and electron microscopy. *Exp. Cell Res.* **221:** 281-288; 1995.

[41] Chattopadhyay, R.; Wiederhold, L.; Szczesny, B.; Boldogh, I.; Hazra, T.; Izumi, T.K.; Mitra, S. Identification and characterization of mitochondrial abasic (AP)-endonuclease in mammalian cells. *Nucleic Acids Res.* **34:** 2067-2076; 2006.

[42] Suh, K.S.; Mutoh, M.; Nagashima, K.; Fernandez-Salas, E.; Edwards, L.E.; Hayes, D.D.; Crutchley, J.M.; Marin, K.G.; Dumont, R.A.; Levy, J.M.; Cheng, C.; Garfield, S.; Yuspa, S.H. The organellar chloride channel protein CLIC4/mtCLIC translocates to the nucleus in response to cellular stress and accelerates apoptosis. *J. Biol. Chem.* **279:** 4632-4641; 2004.

[43] Wang, Y.; Lyu, Y.L.; Wang, J.C. Dual localization of human DNA topoisomerase IIIalpha to mitochondria and nucleus. *Proc. Natl. Acad. Sci. USA.* **99:** 12114-12119; 2002.

[44] Robin, M.A.; Prabu, S.K.; Raza, H.; Anandatheerthavarada, H.K.; Avadhani, N.G. Phosphorylation enhances mitochondrial targeting of GSTA4-4 through increased affinity for binding to cytoplasmic Hsp70. *J. Biol. Chem.* **278:** 18960-18970; 2003.

[45] Vassarotti, A.; Stroud, R.; Douglas, M. Independent mutations at the amino terminus of a protein act as surrogate signals for mitochondrial import. *EMBO J.* **6:** 705-711; 1987.

[46] Lain, B.; Iriarte, A.; Mattingly, J.R.; Moreno, J.I.; Martinez-Carrion, M. Structural features of the

precursor to mitochondrial aspartate aminotransferase responsible for binding to hsp70. *J. Biol. Chem.* **270:** 24732–24739; 1995.

[47] Garry, M.R.; Kavanagh, T.J.; Faustman, E.M.,; Sidhu, J.S.; Liao, R.; Ware, C.; Vliet, P.A.; Deeb, S.S. Sensitivity of mouse lung fibroblasts heterozygous for GPx4 to oxidative stress. *Free Radic. Biol. Med.* **44:** 1075-1087; 2008.

[48] Zimniak, P.; Singhal, S.S.; Srivastava, S.K.; Awasthi, S.; Sharma, R.; Hyden, J.B.; Awasthi, Y.C. Estimation of genomic complexity, heterologous expression, and enzymatic characterization of mouse glutathione S-transferase mGSTA4-4 (GST 5.7). *J. Biol. Chem.* **269:** 992–1000; 1994.

[49] Singhal, S.S.; Zimniak, P.; Awasthi, S.; Piper, J.T.; He, N.G.; Teng, J.I.; Petersen, D.R.; Awasthi, Y.C. Several closely related glutathione S-transferase isozymes catalyzing conjugation of 4-hydroxynonenal are differentially expressed in human tissues. *Arch. Biochem. Biophys.* **311:** 242–250; 1994.

Figure legends

Figure 1. The intracellular distribution of endogenous GSTπ. (A) The intracellular distribution of endogenous GSTπ determined by immunoblotting. Cytosolic, nuclear, and mitochondrial proteins prepared from HCT8, A549, and COS-1 cells. The intracellular distribution of GSTπ determined by immunoblotting as described in the Materials and Methods. Possible contamination by other fractions was checked using antibodies against RCC-1, a marker of nuclear protein, AIF, a marker of mitochondrial protein, and Cu, Zn –SOD, a marker of cytosolic protein, respectively. (B) The mitochondrial distribution of GSTπ determined in detail by immunoblotting using antibodies against RCC-1, AIF, Cu, Zn –SOD, calnexin, a marker of the endoplasmic reticulum, catalase, a marker of peroxisomes, and cathepsin D, a marker of lysosomes. Data represent five independent experiments. (C) Intracellular distribution of endogenous GSTπ evaluated by immunohistochemical analyses. The intracellular distribution of endogenous GSTπ in digitonin-treated cells analyzed by immunohistochemistry using anti-GSTπ antibody as described in the Materials and Methods. The location of the mitochondria was determined by staining the cells with anti-AIF antibody. Fluorescence intensity was observed under a confocal laser scanning microscope. Data represent five independent experiments. (D) Intracellular distribution of endogenous GSTπ evaluated by immunoelectron microscopic analyses. (a) The section was immunoreacted with rabbit anti-GSTπ IgG, followed by colloidal gold (15 nm)-labeled goat anti-rabbit IgG. Colloidal gold particles were seen on the inner membrane (short arrow)

and cristae membrane (long arrow) of the mitochondria. (b) Negative staining control of (a). The section was immunoreacted with normal rabbit IgG, followed by colloidal gold (15 nm) –labeled goat anti-rabbit IgG. (c) Positive staining control of (a). The section was immunoreacted with mouse anti-mitochondria IgG, followed by colloidal gold (10 nm)-labeled goat anti-mouse IgG. Colloidal gold particles were seen on the mitochondria (short and long arrows). (d) Negative staining control of (c). The section was immunoreacted with normal mouse IgG, followed by colloidal gold (10 nm)-labeled goat anti-mouse IgG. Data represent three independent experiments. Bar=200 nm

Figure 2. N-terminal region of GSTπ possesses the mitochondrial targeting signal. (A) Mitochondrial localization of FLAG-tagged GSTπ. The vector pcDNA3/FLAG-GSTπ1-210 was introduced into COS-1 cells with Lipofectamine. After 24h of transfection, the transfectant was harvested, and the cytosolic and mitochondrial proteins were prepared as described in the Materials and Methods. The intracellular distribution of FLAG-GSTπ1-210 in the transfectants was determined by immunoblotting using anti-FLAG and anti-GSTπ antibodies. Possible contamination by other fractions was checked by immunoblot analysis of Cu, Zn –SOD, and AIF. W, wild type; T, transfectant; are indicated. Data represent three independent experiments. (B) Diagrams of GSTπ fragments fused with GFP. (C) Intracellular distribution of

GFP-fused GSTπ fragments. Two micrograms of the expression vector as in (B) was introduced into COS-1 cells grown on glass coverslips with Lipofectamine. After 24h of transfection, the intracellular distribution of GSTπ fragments fused to GFP was analyzed under a confocal laser scanning microscope. The location of the mitochondria was determined by staining the cells with MitoRed. Data represent three independent experiments. **(D)** The arginine residues in the MTS are required for the mitochondrial localization of GSTπ. Mutations from arginine to alanine in the GSTπ1-84 region of pcDNA3.1/GSTπ1-84-GFP were generated by site-directed mutagenesis as described in the Materials and Methods. Two micrograms of pcDNA3.1/GSTπ1-84-GFP with or without mutations was introduced into COS-1 cells. After 24h of transfection, the intracellular distribution of GSTπ1-84-GFP mutants was analyzed under a confocal laser scanning microscope as described in the Materials and Methods. The location of the mitochondria was determined by staining the cells with MitoRed. Data represent three independent experiments. (E) pcDNA3.1/GSTπ1-210-myc (wild type) and pcDNA3.1/GSTπ1-210-myc (mutation from arginine to alanine at positions 12,14,19,71, and 75) were introduced into COS-1 cells. After 24h of transfection, the transfectants were harvested, and the mitochondrial proteins were prepared as described in the Materials and Methods. The mitochondrial localization of myc-tagged GSTπ with or without mutation in the transfectants was evaluated by immunoblotting using anti-GSTπ, anti-myc, and anti-AIF antibodies. Possible contamination

by other fractions was checked by immunoblotting for calnexin, catalase, and cathepsin D. Data represent three independent experiments.

Figure 3. The overexpression of GSTπ diminishes the cytotoxicity and the loss of mitochondrial membrane potential induced by inhibitors for the mitochondrial respiratory chain. (A) Expression of GSTπ in mock-transfected (VecC-12) and GSTπgene–transfected (FHGC-16) HCT8 cells. The expression levels of endogenous GSTπ and FLAG-HA-tagged GSTπ1-210 in the cytosol, nucleus, and mitochondrial fraction were estimated by immunoblotting using anti-GSTπ antibodies as described in the Materials and Methods. Antibodies against RCC-1, AIF, and Cu, Zn –SOD were used for the loading control (upper panel). Data represent three independent experiments. Total GST activity with lysates from the cytosol, the nucleus, and mitochondria were assayed as described in the Materials and Methods (lower panel). Data are shown as a percentage of that of parental HCT8 cells, and presented as the mean ± S.D. for three independent experiments. *, $p<0.05$ compared with VecC-12 cells. (B) The overexpression of GSTπ diminishes the cytotoxicity of inhibitors for the mitochondrial respiratory chain. FHGC-16 and VecC-12 cells were treated with various concentration of rotenone, antimycin A, or potassium cyanide for 24 h, and cell viability was estimated by the MTT assay as described in the Materials and Methods. Data for each MTT assay were expressed as a

percentage of that just before the treatment with mitochondrial inhibitors. Each value represents the mean ± S.D. for three independent experiments. Open symbol, VecC-12 cells; closed symbol, FHGC-16 cells. *, $p<0.05$ compared with VecC-12 cells. (C) There is no detectable difference in superoxide generation between FHGC-16 and VecC-12 cells treated with rotenone or antimycin A. FHGC-16 and VecC-12 cells were treated with 350 μM rotenone, 150 μM antimycin A or 5 mM potassium cyanide for the periods indicated. Then, detection of mitochondrial superoxide generated by these chemicals in FHGC-16 and VecC-12 cells was performed with flow cytometry using MitoSOX Red as described in the Materials and Methods. Data represent three independent experiments. (D) The overexpression of GSTπ prevents the loss of mitochondrial membrane potential induced by antimycin A. FHGC-16 and VecC-12 cells were treated with 150 μM antimycin A for the periods indicated. The alteration of mitochondrial membrane potential was examined by flow cytometry using rhodamine 123 as described in the Materials and Methods. Data represent three independent experiments.

Figure 4. GSTπ-targeting siRNA enhances the loss of mitochondrial membrane potential and cytotoxicity of inhibitors for the mitochondrial respiratory chain. (A) GSTπ was silenced using a pre-designed GSTπ-targeting siRNA. The GSTπ-targeting or negative control siRNA was introduced into FHGC-16 and

VecC-12 cells. The cells were incubated for an additional 48 h, and the expression of GSTπ in the isolated mitochondrial fraction was analyzed by immunoblotting using anti-GSTπ antibody. Anti-AIF antibodies were used for the loading control (upper panel). Data represent three independent experiments. Total GST activity of the isolated mitochondrial fraction was assayed (lower panel). Data are shown as a percentage of that of the untreated cells, and presented as the mean ± S.D. for three independent experiments. *, $p<0.05$ compared with transfection of the negative control siRNA. (B) GSTπ-targeting siRNA enhances the loss of mitochondrial membrane potential induced by antimycin A. The GSTπ-targeting or negative control siRNA was introduced into VecC-12 cells. The cells were incubated for an additional 48 h, and then treated with 150μM antimycin A for 24 h. The alteration of mitochondrial membrane potential was examined by flow cytometry using rhodamine 123. Data represent three independent experiments. (C) GSTπ-targeting siRNA enhances the cytotoxicity of antimycin A. GSTπ-targeting or negative control siRNA was introduced into FHGC-16 and VecC-12 cells. These cells were incubated for an additional 48 h, and then treated with various concentrations of antimycin A for 24 h. Cell viability was estimated by the MTT assay. Data were expressed as a percentage of that without antimycin A. Each value represents the means ± S.D. for three independent experiments. Open symbol, cells transfected with negative control siRNA; closed symbol, cells transfected with GSTπ-targeted siRNA. *, $p<0.05$ compared with cells transfected with negative control

siRNA.

Supplemental Figure 1. Intracellular distribution of GFP-fused GSTπ fragments. Two micrograms of the expression vector as in Fig.3B was introduced into COS-1 cells grown on glass coverslips with Lipofectamine. After 24h of transfection, the intracellular distribution of GSTπ fragments fused to GFP was analyzed under a confocal laser scanning microscope. The location of the mitochondria was determined by staining the cells with MitoRed. Data represent three independent experiments.

Supplemental figure 2. Mutations from arginine to alanine in the GSTπ1-84 region of pcDNA3.1/GSTπ1-84-GFP were generated by site-directed mutagenesis. Two micrograms of pcDNA3.1/GSTπ1-84-GFP with or without mutations was introduced into COS-1 cells. After 24h of transfection, the intracellular distribution of GSTπ1-84-GFP mutants was analyzed under a confocal laser scanning microscope. The location of the mitochondria was determined by staining the cells with MitoRed. Data represent three independent experiments.

Supplemental figure 3. Overexpression of GSTπ diminishes the cytotoxicity of inhibitors for the

mitochondrial respiratory chain. FHGC-16 and VecC-12 cells were treated with various concentrations of rotenone, antimycin A, or potassium cyanide for 24 h, and cell viability was estimated by the LDH assay as described in the Materials and Methods. Data for each LDH assay were expressed as a percentage of that just before the treatment with mitochondrial inhibitors. Each value represents the mean ± S.D. for three independent experiments. Open symbol, VecC-12 cells; closed symbol, FHGC-16 cells. *, $p<0.05$ compared with VecC-12 cells.

Supplemental figure 4. GSTπ-targeting siRNA enhances the cytotoxicity of antimycin A. GSTπ-targeting or negative control siRNA was introduced into FHGC-16 and VecC-12 cells. These cells were incubated for an additional 48 h, and then treated with various concentrations of antimycin A for 24 h. Cell viability was estimated by the LDH assay. Data for each LDH assay were expressed as a percentage of that just before the treatment with mitochondrial inhibitors. Each value represents the mean ± S.D. for three independent experiments. Open symbol, cells transfected with negative control siRNA; closed symbol, cells transfected with GSTπ-targeted siRNA. *, $p<0.05$ compared with transfectants with negative control siRNA.

The supplemental section

Materials and Methods

Materials- RPMI 1640 medium and Dulbecco's modified Eagle's medium (DMEM) were purchased from Sigma Aldrich (St. Louis, MO); fetal bovine serum (FBS) was from Invitrogen Corp. (Carlsbad, CA); horseradish peroxidase (HRP)-labeled anti-mouse IgG, HRP-labeled anti-rabbit IgG, and HRP-labeled anti-goat IgG were from DAKO A/S (Glostrup, Denmark); fluorescein isothiocyanate (FITC)-conjugated anti-rabbit IgG and rhodamine-conjugated anti-mouse IgG were from ICN Pharmaceuticals (Aurora, OH); anti-green fluorescent protein (GFP) antibody was from Invitrogen Corp.; anti-FLAG antibody was from Sigma Aldrich; anti-myc antibody was from Upstate (Charlottesville, VA); anti-human regulator of chromosome condensation 1 (RCC1) antibody was from BD Biosciences Pharmingen (San Jose, CA); anti-human apoptosis–inducing factor (AIF) antibody and anti-human cathepsin D were from Santa Cruz Biotechnology, Inc. (Santa Cruz, CA); anti-human calnexin was from Stressgen (Victoria, BC, Canada); and anti-human catalase was from CALBIOCHEM (San Diego, CA). Anti-human Cu, Zn-superoxide dismutase (Cu, Zn-SOD) antibody and Mn-superoxide dismutase (Mn-SOD) antibody were a gift from Dr. K. Suzuki (Hyogo College of Medicine, Nishinomiya, Japan). The Slow Fade Light Antifade kit, lipofectamine reagent,

lipofectamine 2000, pcDNA3.1/CT-GFP vector, pcDNA3.1/*myc*-HisA vector, MitoSOX Red, and rhodamine 123 were purchased from Invitrogen Corp. The FLAG-HA-tagged protein expression vector (pcDNA3/FLAG-HA), constructed by introducing a *Bgl*II-Kozack-ATG-FLAG-HA-*EcoR*I fragment into *Bam*HI-*Eco*RI restriction sites of pcDNA3 (Invitrogen), was a gift from Dr. J. Yanagisawa (Institute of Applied Biochemistry, University of Tsukuba, Ibaraki, Japan). The QuickChange Site-Directed Mutagenesis Kit was purchased from STRATAGENE (La Jolla, CA). GSTπ-targeting siRNA and negative control (scramble) siRNA were from HAYASHI KASEI Co. (Osaka, Japan). The Enhanced Chemiluminescence (ECL) kit and Percoll were purchased from GE Healthcare Bio-Sciences (Little Chalfont, UK). Digitonin was from CALBIOCHEM (San Diego, CA). 9-[2-(4'-Methylcoumarin-7'-oxycarbonyl) phenyl]-3, 6-bis (diethylamino) xanthylium chloride (*Cellstain*-MitoRed) was from DOJINDO (Kumamoto, Japan). Other chemicals and reagents were purchased from Sigma Aldrich. The Lactate dehydrogenase (LDH) assay kit (MTX-LDH) was purchased from KYOKUTO PHARMACEUTICAL INDUSTRIAL Co. (Tokyo, Japan).

Cells culture- We used the cancer cell lines HCT8 (human colonic carcinoma), A549 (human lung adenocarcinoma), and COS-1 (African green monkey, kidney). Dr. K. J. Scanlon (Berlex Biosciences, CA) donated the HCT8 cells and Dr. H. Isobe (Hokkaido University School of Medicine, Sapporo, Japan), the

A549 cells. COS-1 cells were purchased from American Type Culture Collection (Rockville, MD). The COS-1 cells were maintained in DMEM, and the other cells, in RPMI 1640 medium, supplemented with 10% FBS at 37^{o}C under a humidified atmosphere of 5% CO_2.

Construction of vectors for protein expression- The GSTπ cDNA was prepared by a reverse transcription polymerase chain reaction (PCR) method using total RNA extracted from HCT8 cells as described previously (17). To create GSTπ1-44-GFP, GSTπ1-60-GFP, GSTπ1-70-GFP, GSTπ1-84-GFP, and GSTπ20-84-GFP, GSTπ fragments were prepared by PCR using GSTπ cDNA as a template and an appropriate set of primers. The primers used were as follows: GSTπ1-44 sense, 5'-ACC GAA TTC GCC ACC ATG CCG CCC TAC ACC GTG GTC; GSTπ1-44 antisense, 5'- GCG GAT ATC TGA GTG AGC CCT CCT GCC ACG TCT C; GSTπ1-60 sense, 5'-ACC GAA TTC GCC ACC ATG CCG CCC TAC ACC GTG GTC; GSTπ1-60 antisense, 5'-GCG GAT ATC GGT CTC CGT CCT GGA ACT TGG G; GSTπ1-70 sense, 5'-ACC GAA TTC GCC ACC ATG CCG CCC TAC ACC GTG GTC; GSTπ1-70 antisense, 5'- GCG GAT ATC GCA GGA TGG TAT TGG ACT GGT A; GSTπ1-84 sense, 5'-ACC GAA TTC GCC ACC ATG CCG CCC TAC ACC GTG GTC; GSTπ1-84 antisense, 5'-GCG GAT ATC GGT CCT TCC CAT AGA GCC CAA G; GSTπ20-84 sense, 5'-ACC GAA TTC GCC ACC ATG CTG CTG GCA GAT CAG GGC; GSTπ20-84 antisense, 5'- GCG GAT ATC GGT CCT TCC

CAT AGA GCC CAA G. Following digestion with *Eco*RI and *Eco*RV, the resulting PCR products were subcloned into the *Eco*RI-*Eco*RV restriction sites of pcDNA3.1/CT-GFP.

To obtain a full-length GSTπ tagged at the N-terminal with FLAG-HA or at the C-terminal with *myc*-His, GSTπ cDNA was prepared by PCR using an appropriate set of primers. The following primers were used: FLAG-HA-GSTπ1-210 sense, 5'-CTC GCG GCC GCA AAT GCC GCC CTA CAC CGT GGT C; FLAG-HA-GSTπ1-210 antisense, 5'- ATA GGG CCC TCA CTG TTT CCC GTT GCC ATT GAT; GSTπ1-210-*myc* sense, 5'-ACC AAG CTT CTG CCA CCA TGC CGC CCT ACA CCG TGG TC; GSTπ1-210-*myc* antisense, 5'-GCG TCT AGG CTG TTT CCC GTT GCC ATT GAT. The PCR products were digested with *Not*I and *Apa*I and subcloned into pcDNA3/FLAG-HA or digested with *Hind*III and *Xba*I and subcloned into pcDNA3.1/*myc*-His A. All newly constructed vectors were transformed into a JM109 *Escherichia coli* host and purified using a GeneElute Hp plasmid midiprep kit (Sigma Aldrich). The nucleotide sequences of all constructs were determined using the CEQ DTCS-Quick Start kit on a CEQ 8000 Genetic Analysis System (Beckman Coulter, Fullerton, CA).

Generation of mutants- A point mutation in the region of GSTπ1-84 was generated by site-directed mutagenesis with pcDNA3.1/GSTπ1-84-GFP or pcDNA3.1/GSTπ1-210-*myc* as a template. The mutants were

generated using a QuickChange Site-Directed Mutagenesis Kit with overlapping primers containing the desired mutation. The primers used were as follows: GSTπR12A sense, 5'-CC GTG GTC TAT TTC CCA GTT GCC GGC CGC TGC GCG GCC CTG CGC; GSTπR12A antisense, 5'-GCG CAG GGC CGC GCA GCG GCC GGC AAC TGG GAA ATA GAC CAC GG; GSTπR14A sense, 5'-GTC TAT TTC CCA GTT CGA GGC GCC TGC GCG GCC CTG CGC ATG CTG; GSTπR14A antisense, 5'-CAG CAT GCG CAG GGC CGC GCA GGC GCC TCG AAC TGG GAA ATA GAC; GSTπR19A sense, 5'-C TGC GCG GCC CTG GCC ATG CTG CTG GCA G; GSTπR19A antisense, 5'-C TGC CAG CAG CAT GGC CAG GGC CGC GCA G; GSTπR71A sense, 5'-CC AAT ACC ATC CTG GCC CAC CTG GGC CGC ACC CTT GGG CTC TAT G; GSTπR71A antisense, 5'-C ATA GAG CCC AAG GGT GCG GCC CAG GTG GGC CAG GAT GGT ATT GG; GSTπR75A sense, 5'-CC AAT ACC ATC CTG CGT CAC CTG GGC GCC ACC CTT GGG CTC TAT G; GSTπR75A antisense, 5'-C ATA GAG CCC AAG GGT GGC GCC CAG GTG ACG CAG GAT GGT ATT GG; The nucleotide sequences of all constructs were determined using the CEQ DTCS-Quick Start kit on a CEQ 8000 Genetic Analysis System.

Figure 1.

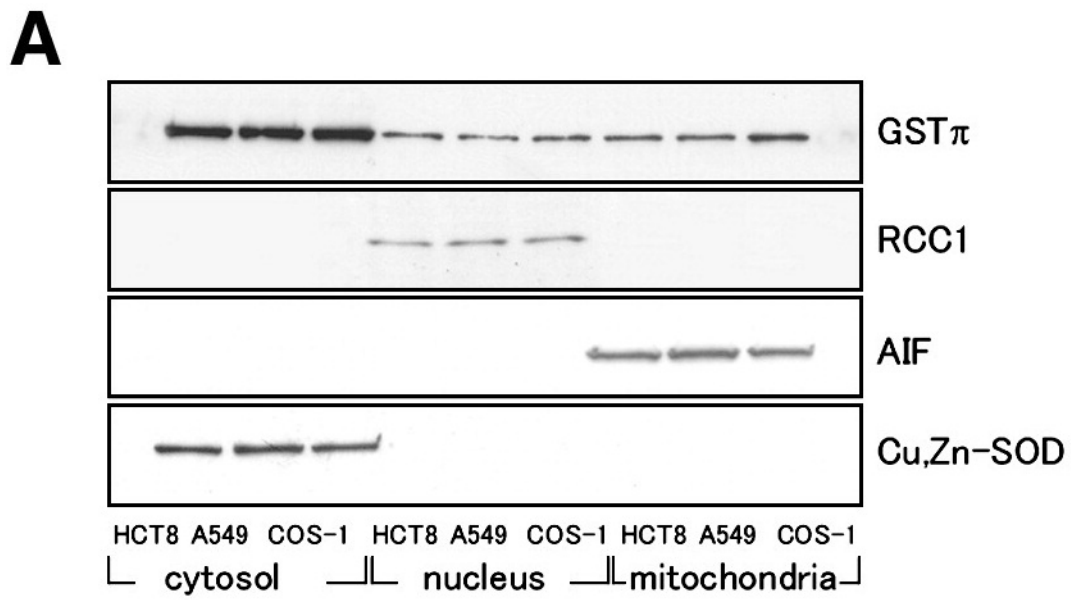
A
GSTπ
RCC1
AIF
Cu,Zn-SOD
HCT8 A549 COS-1 HCT8 A549 COS-1 HCT8 A549 COS-1
cytosol
nucleus
mitochondria

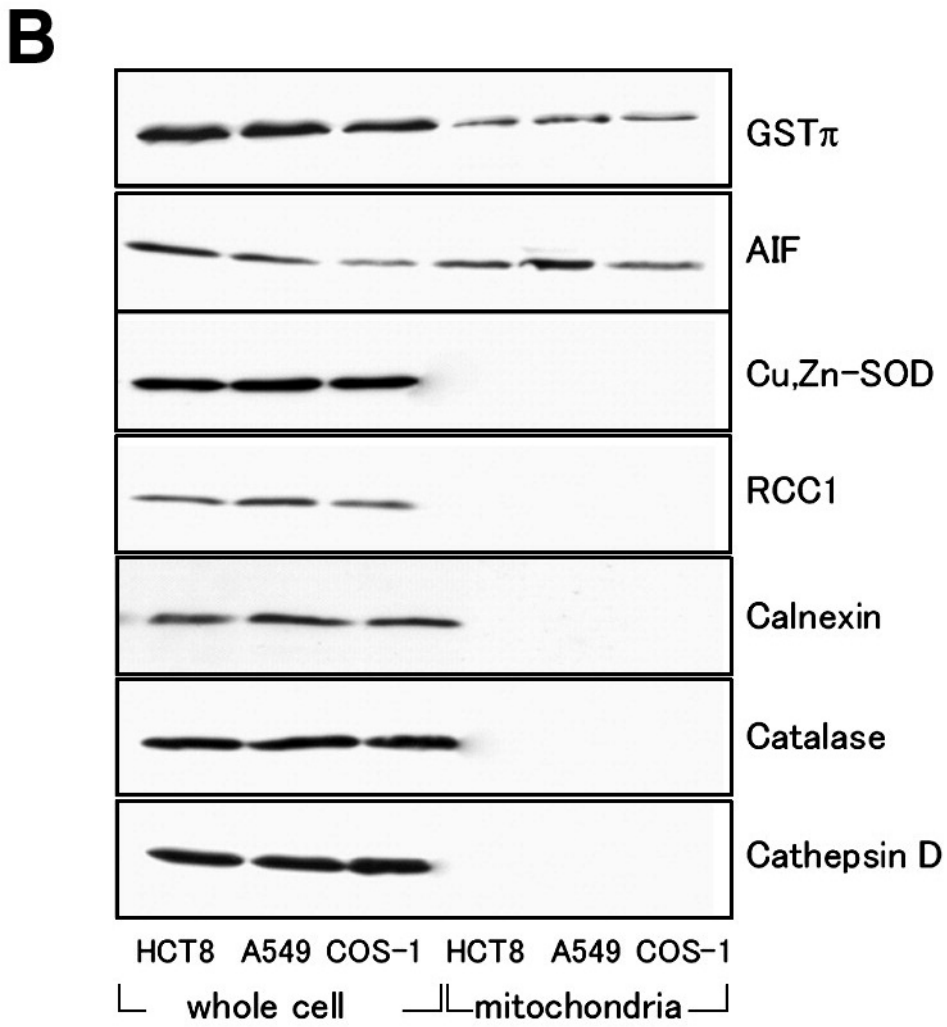
B
GSTπ
AIF
Cu,Zn-SOD
RCC1
Calnexin
Catalase
Cathepsin D
HCT8 A549 COS-1 HCT8 A549 COS-1
whole cell
mitochondria

Figure 1.

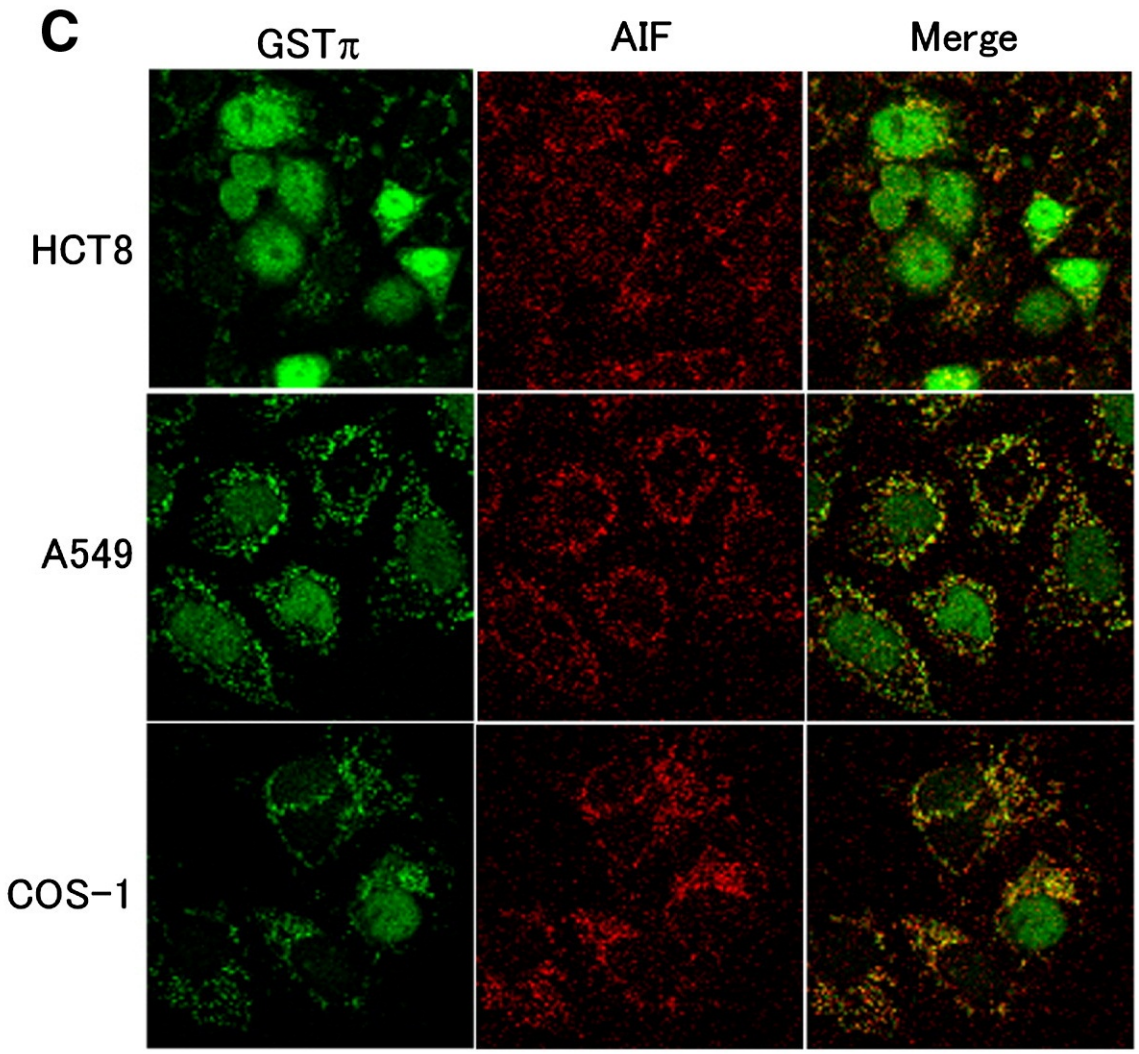

Figure 1.

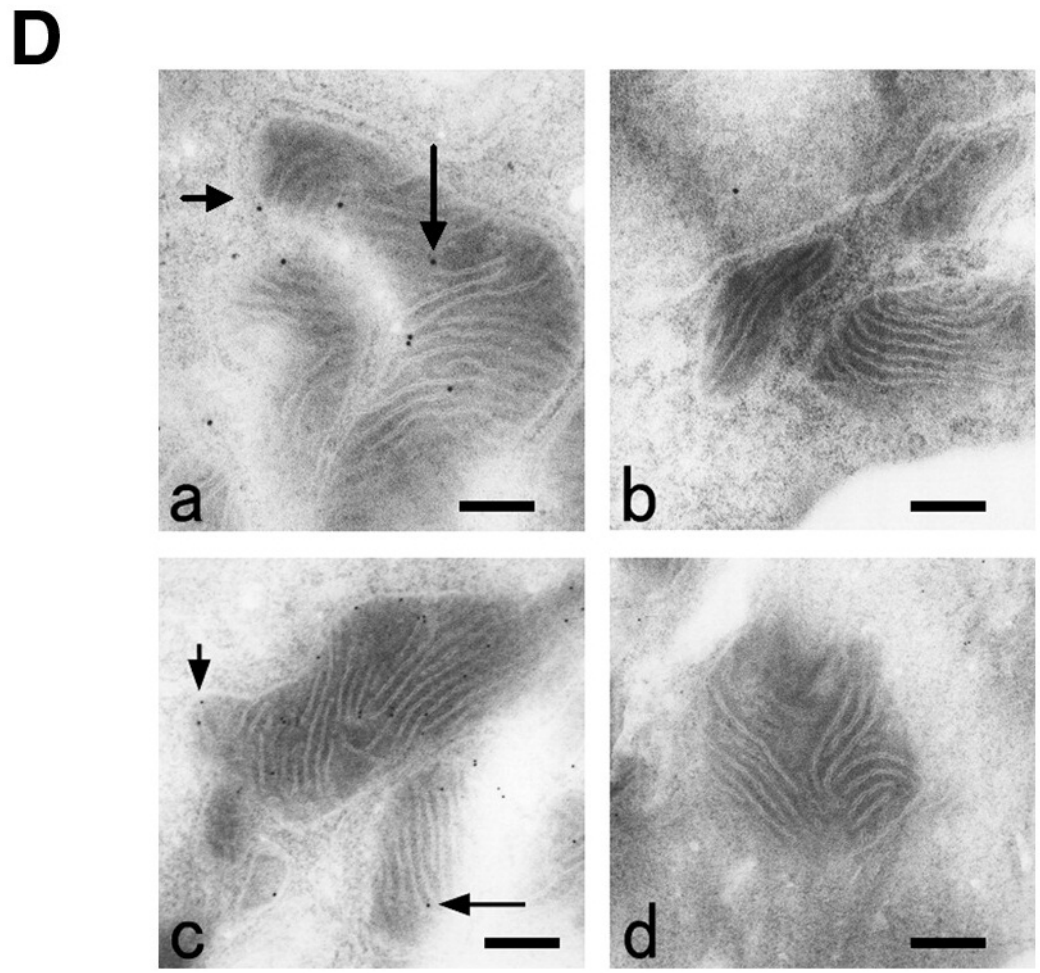

Figure 2.

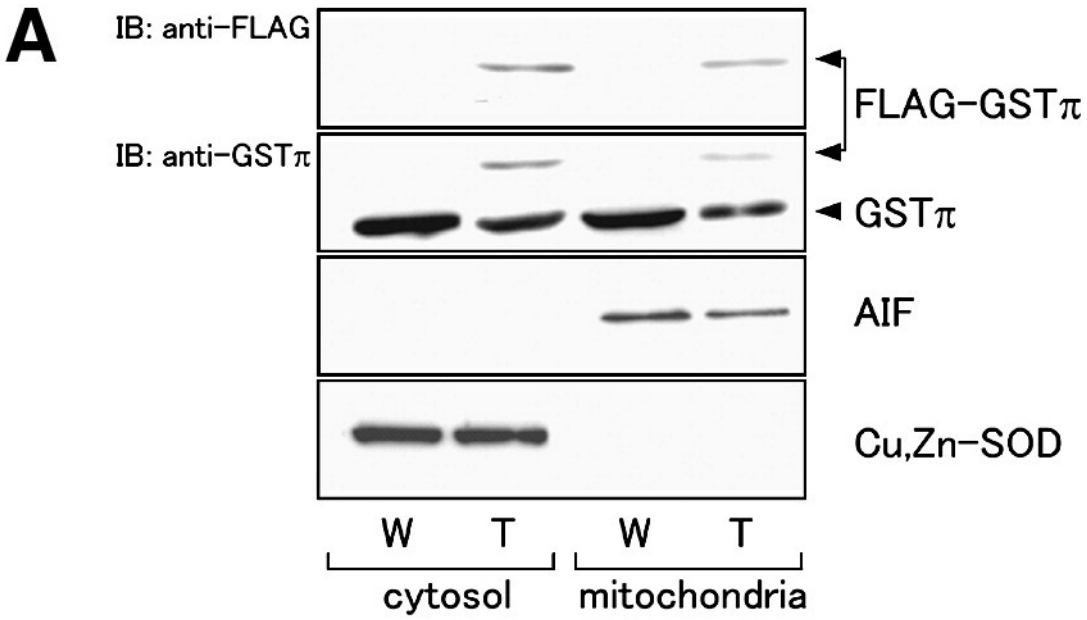
A
IB: anti-FLAG
IB: anti-GSTπ
FLAG-GSTπ
GSTπ
AIF
Cu,Zn-SOD
W
T
W
T
cytosol
mitochondria

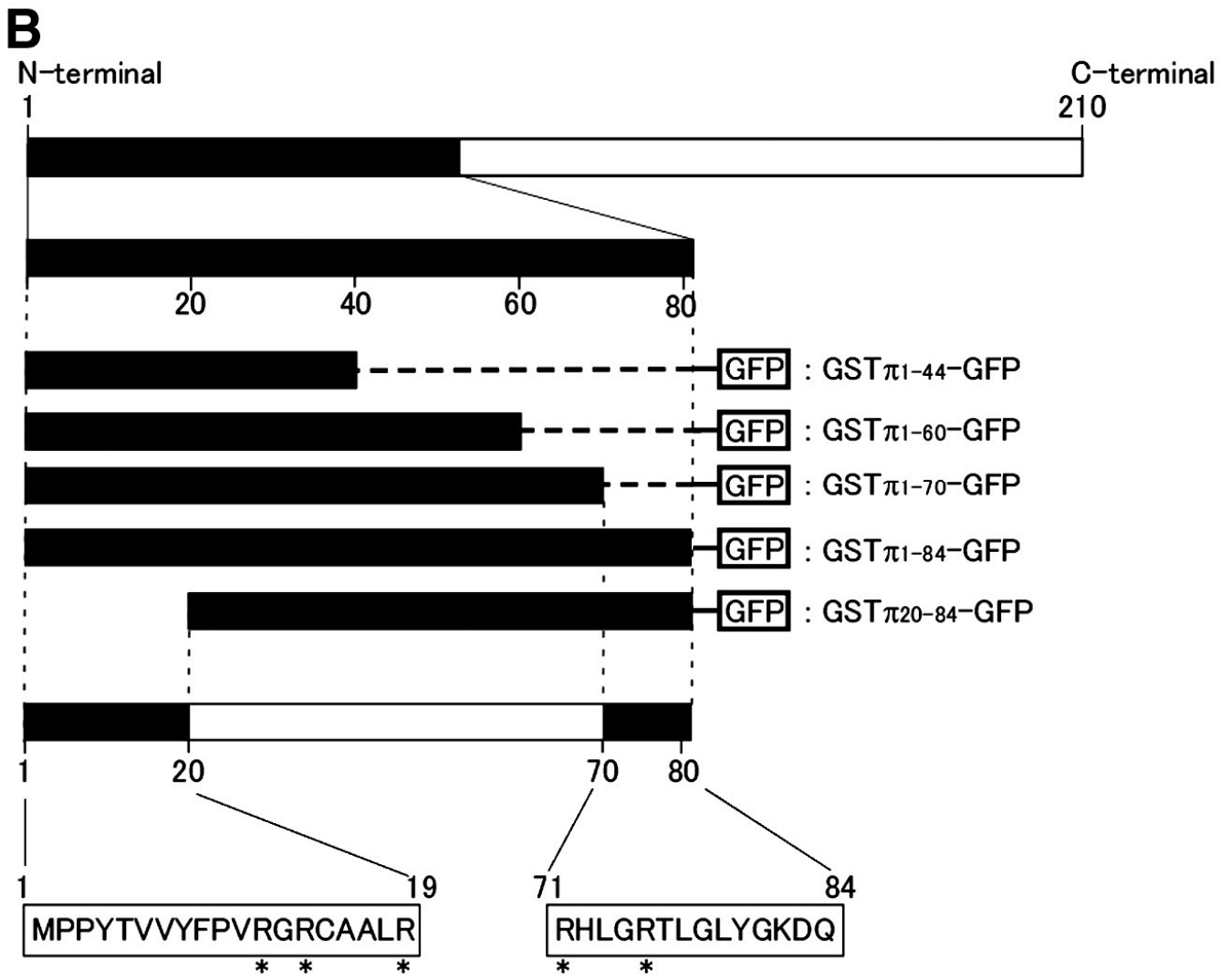
B
N-terminal
C-terminal
1
210
20
40
60
80
GFP : GSTπ1-44-GFP
GFP : GSTπ1-60-GFP
GFP : GSTπ1-70-GFP
GFP : GSTπ1-84-GFP
GFP : GSTπ20-84-GFP
1
20
70
80
1
19
71
84
MPPYTVVYFPVRGRCAALR
RHLGRTLGLYGKDQ
* * *
* *

Figure 2.

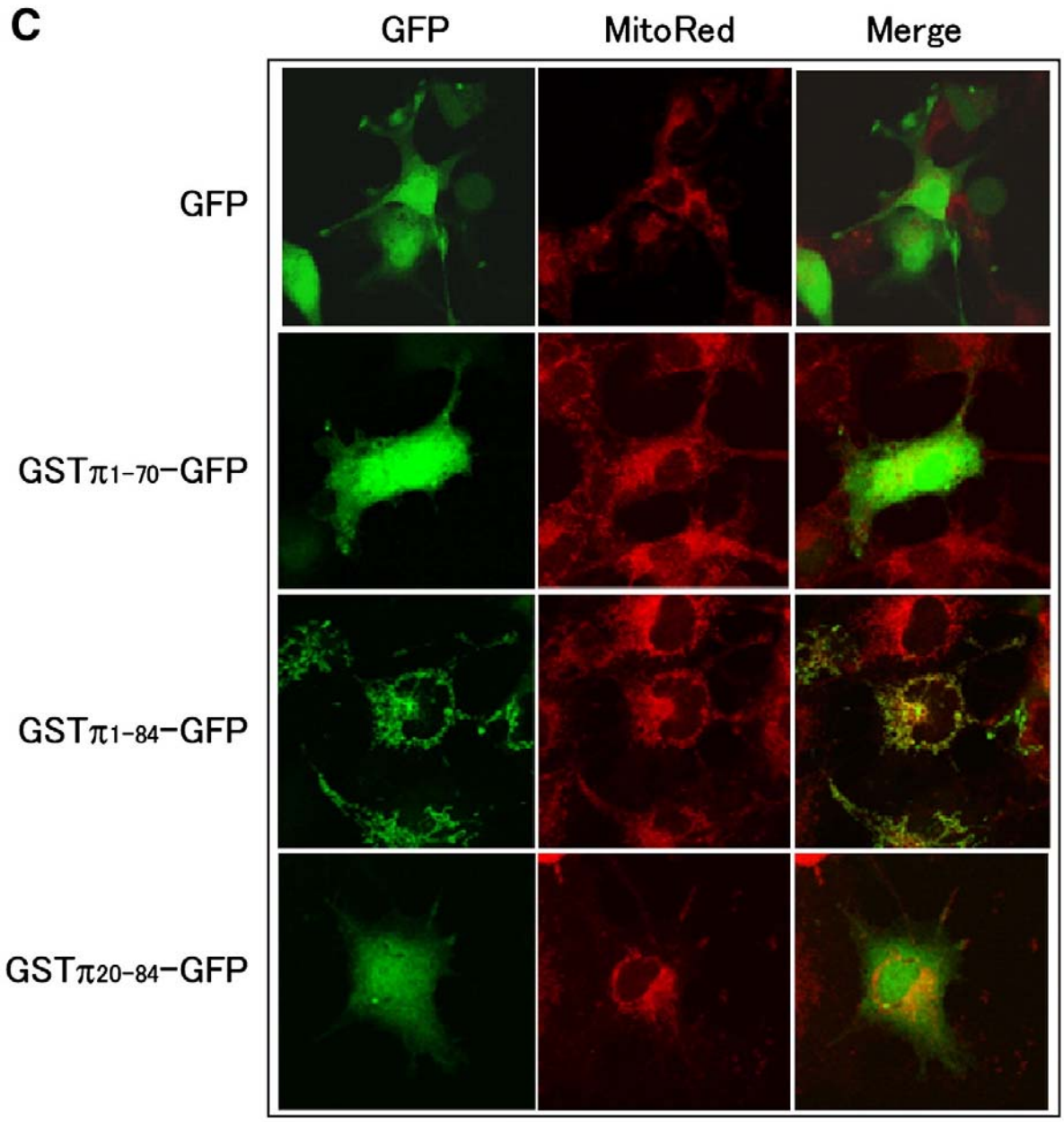
C
GFP
MitoRed
Merge
GFP
GSTπ1-70-GFP
GSTπ1-84-GFP
GSTπ20-84-GFP

Figure 2.

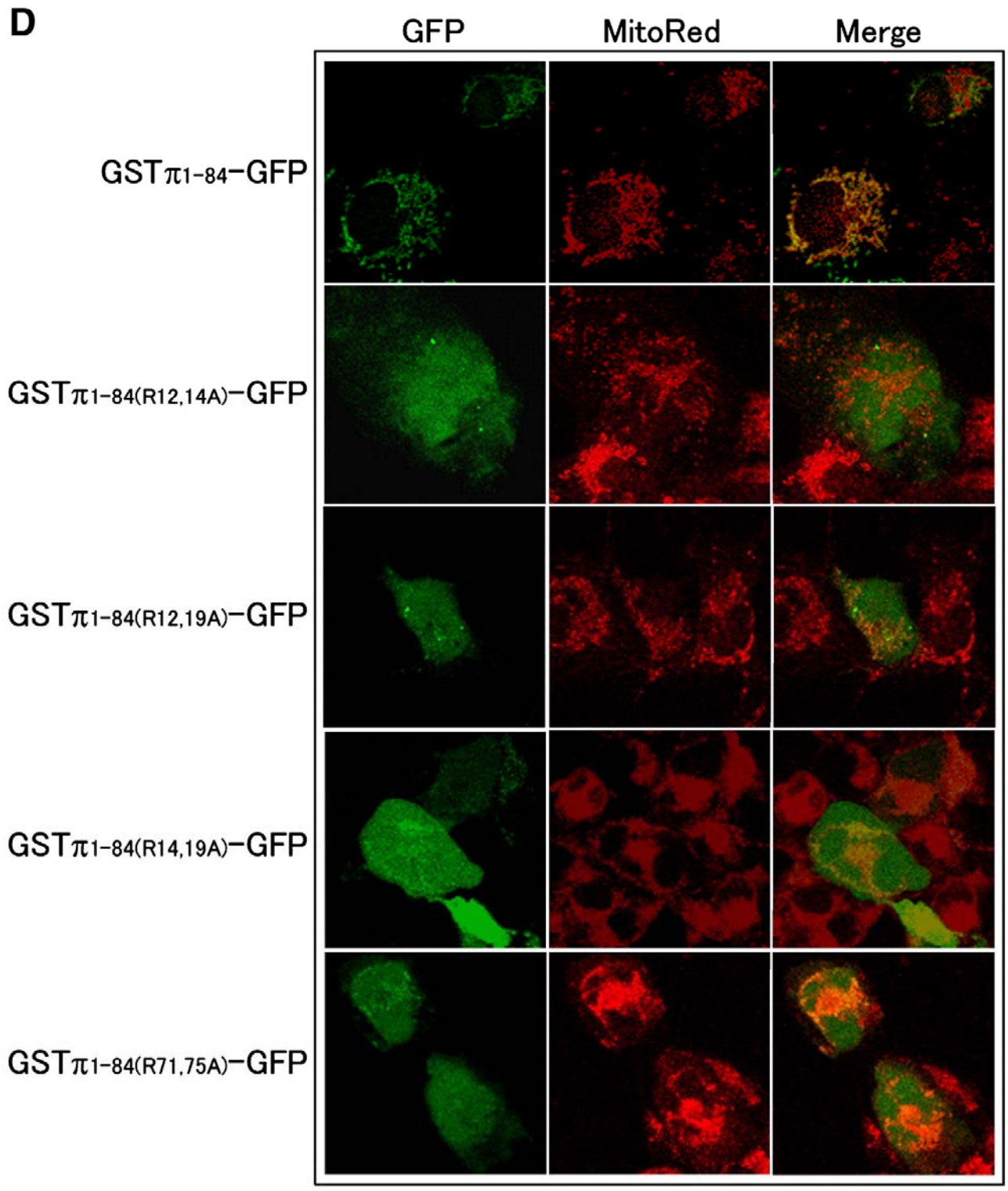
D
GFP
MitoRed
Merge
GSTπ1-84−GFP
GSTπ1-84(R12,14A)−GFP
GSTπ1-84(R12,19A)−GFP
GSTπ1-84(R14,19A)−GFP
GSTπ1-84(R71,75A)−GFP

Figure 2.

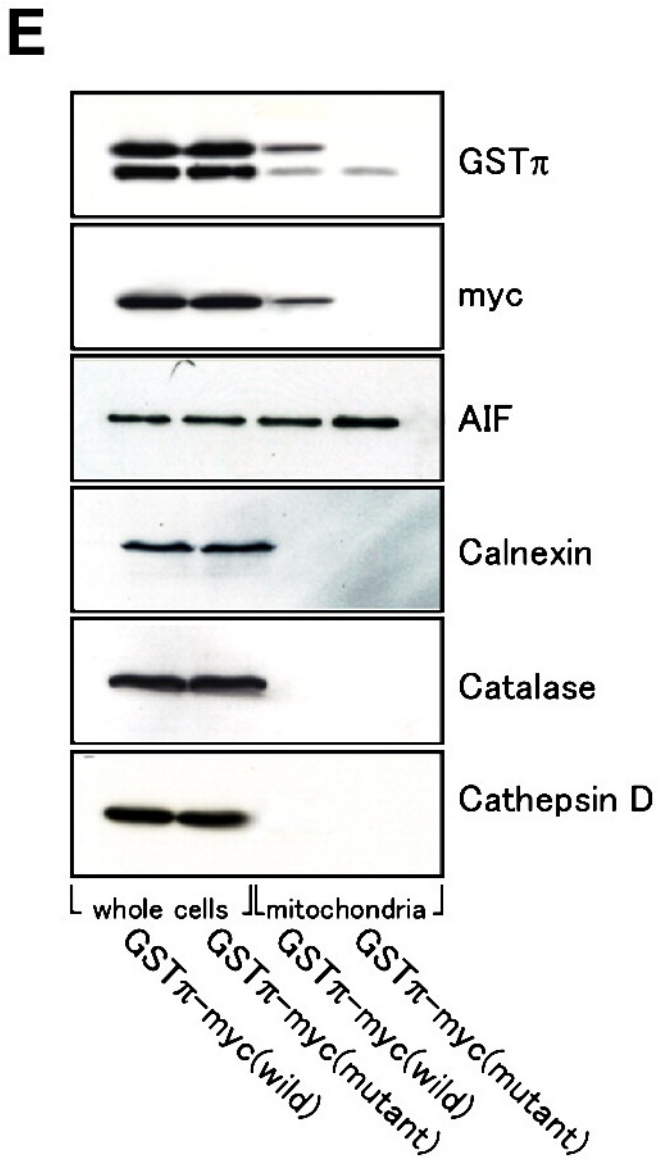
E
GSTπ
myc
AIF
Calnexin
Catalase
Cathepsin D
whole cells
mitochondria
GSTπ-myc(wild)
GSTπ-myc(mutant)
GSTπ-myc(wild)
GSTπ-myc(mutant)

Figure 3.

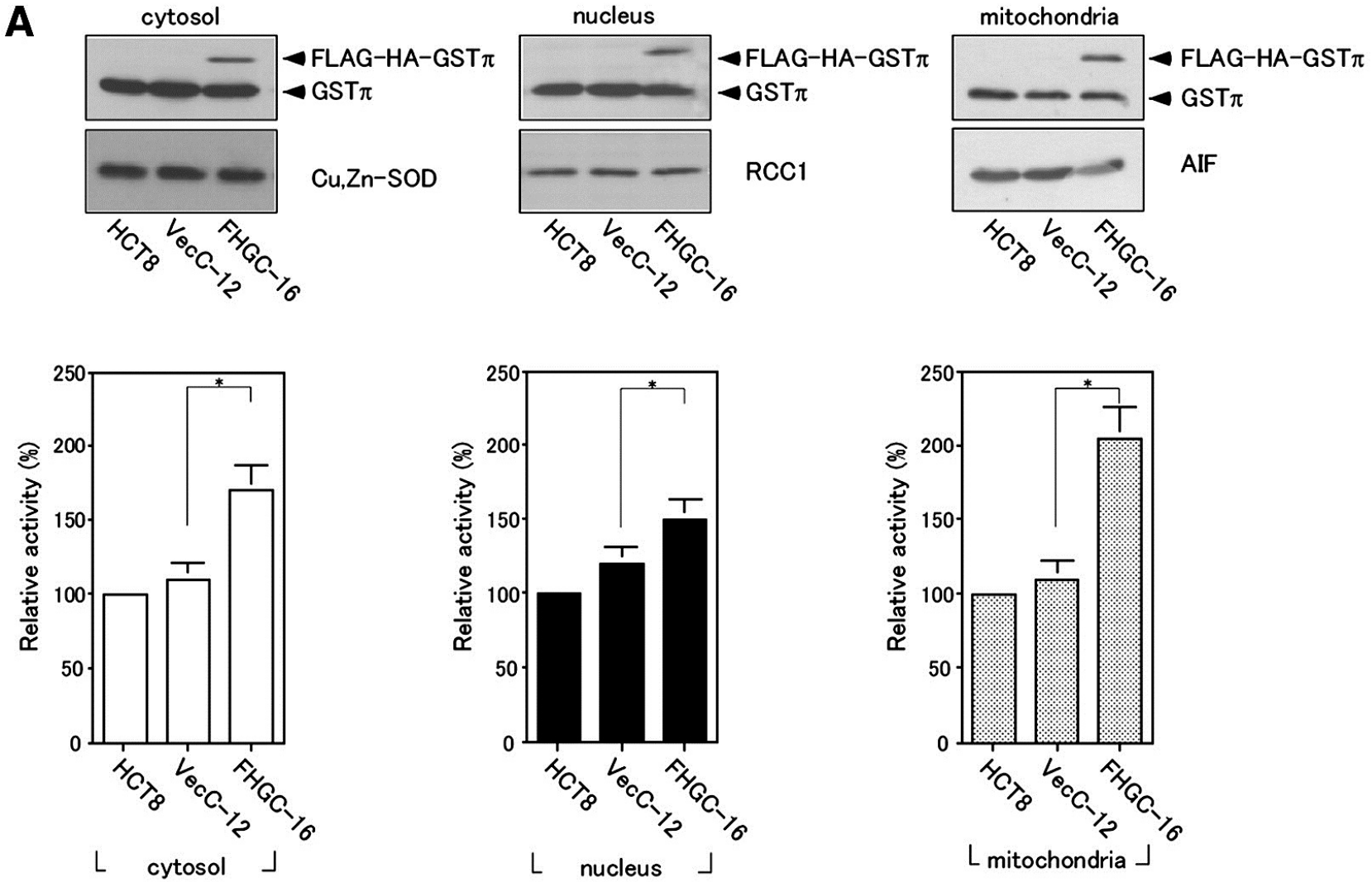
A
cytosol
nucleus
mitochondria
FLAG-HA-GSTπ
GSTπ
Cu,Zn-SOD
RCC1
AIF
HCT8
VecC-12
FHGC-16
Relative activity (%)
250
200
150
100
50
0
*
cytosol
nucleus
mitochondria

Figure 3.

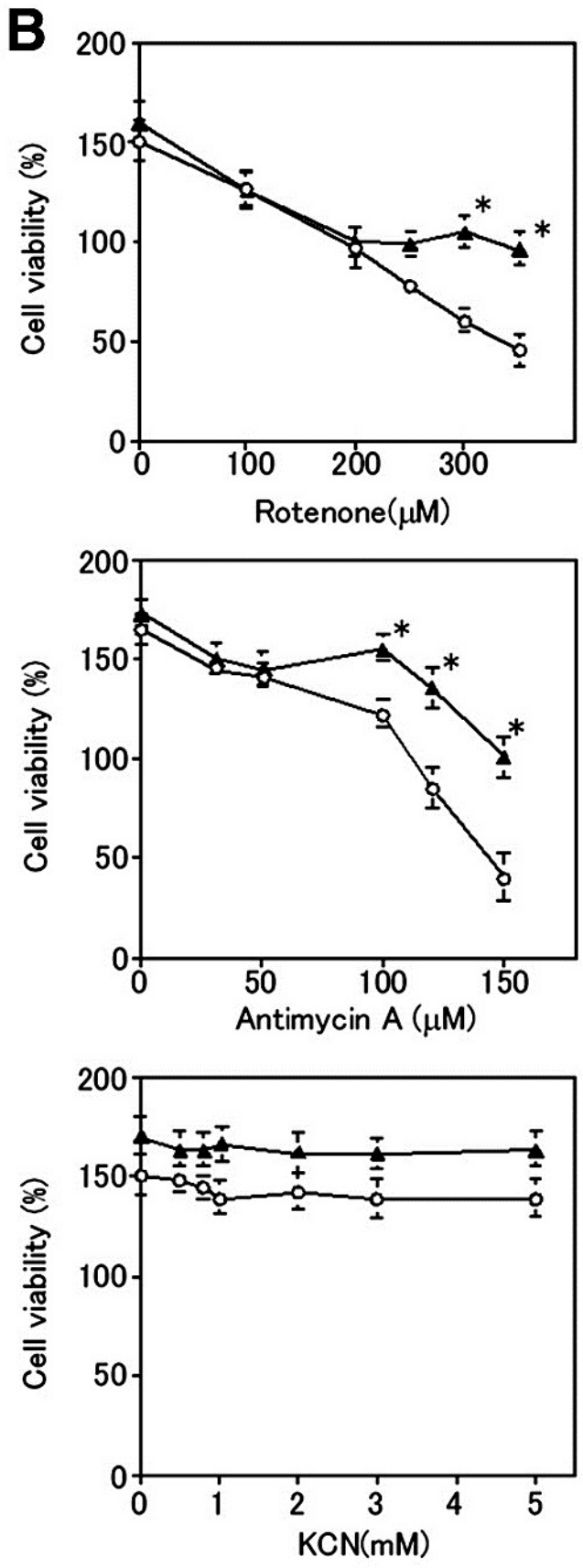
B
Cell viability (%)
200
150
100
50
0
0
100
200
300
Rotenone(μM)
Cell viability (%)
200
150
100
50
0
0
50
100
150
Antimycin A (μM)
Cell viability (%)
200
150
100
50
0
0
1
2
3
4
5
KCN(mM)

Figure 3.

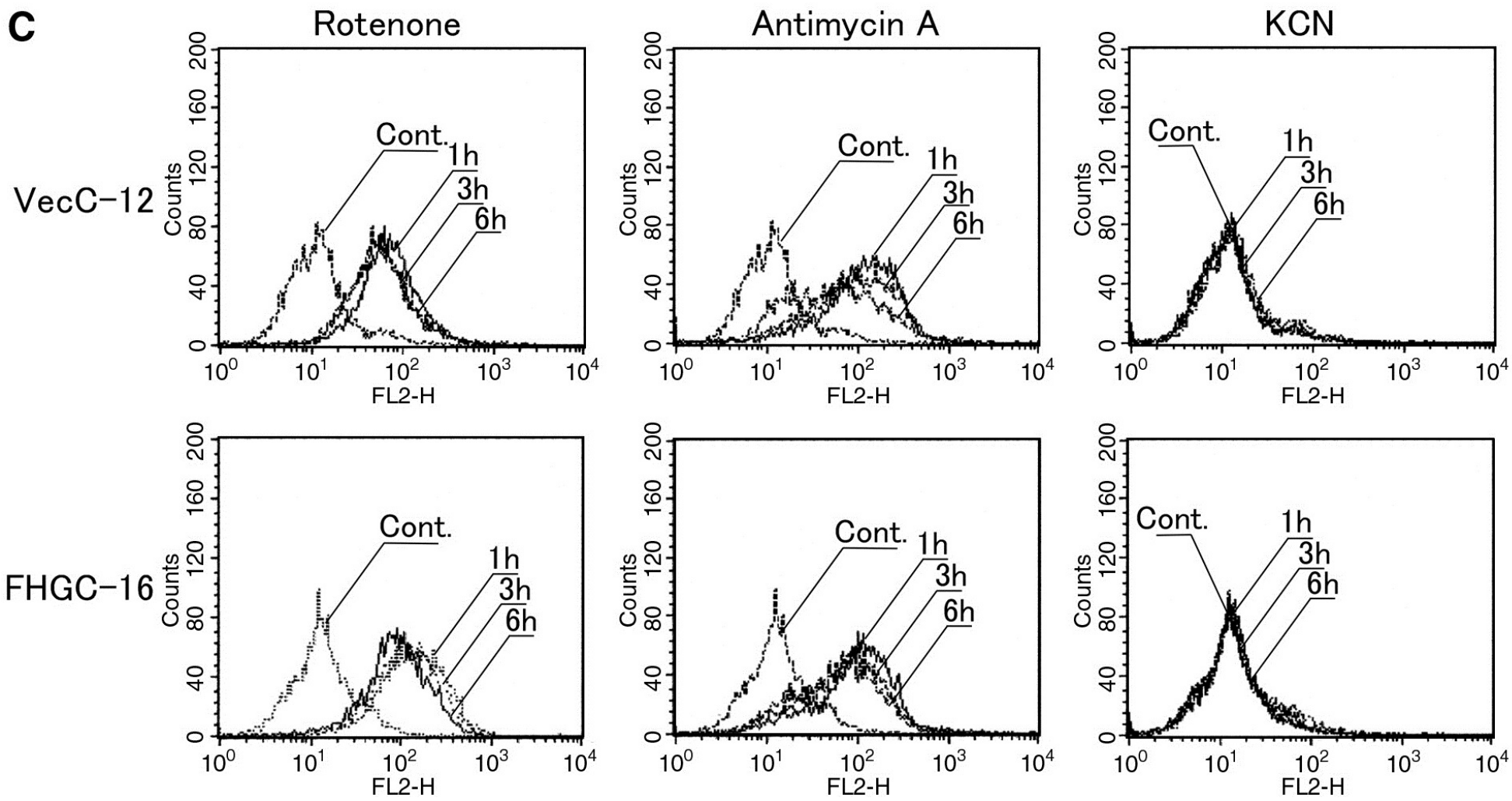
C
Rotenone
Antimycin A
KCN
VecC-12
FHGC-16
Cont.
1h
3h
6h
Counts
FL2-H

Figure 3.

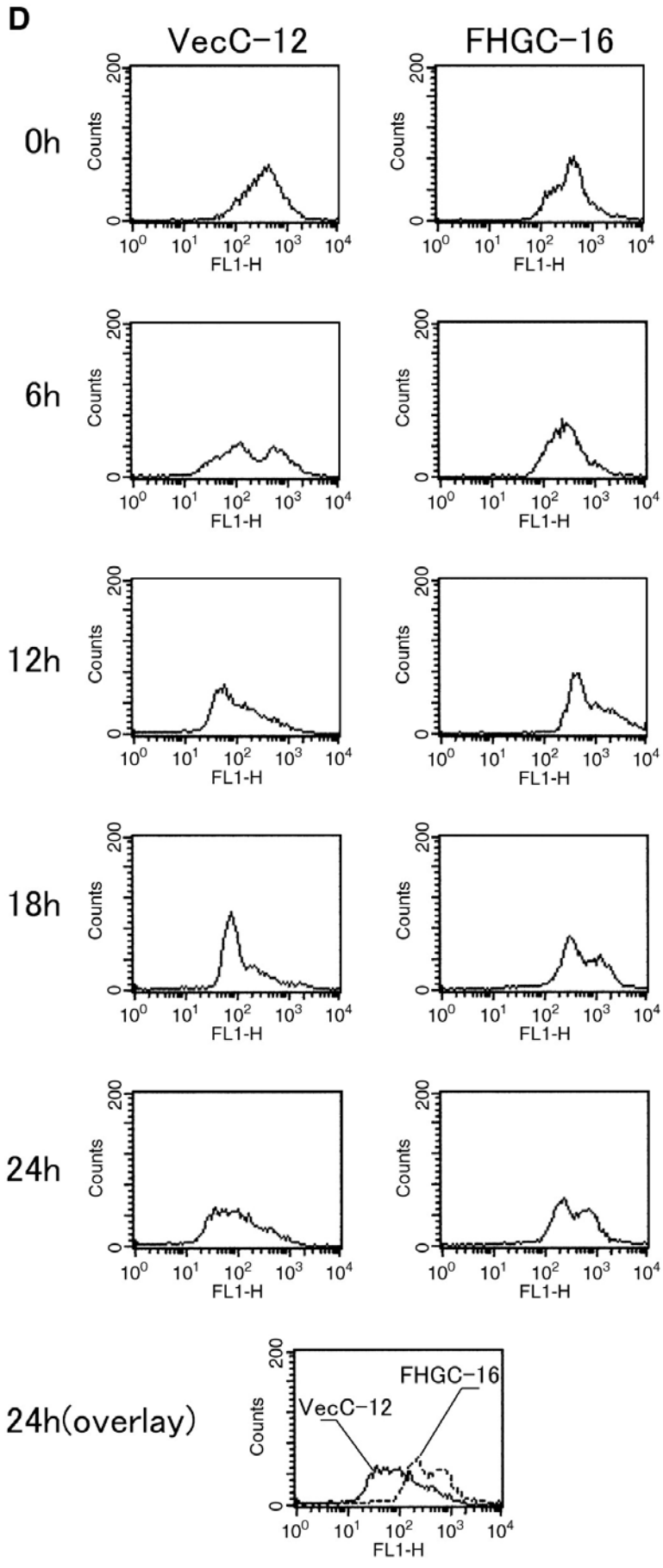
D
VecC-12
FHGC-16
0h
6h
12h
18h
24h
24h(overlay)
Counts
FL1-H
FHGC-16
VecC-12

Figure 4.

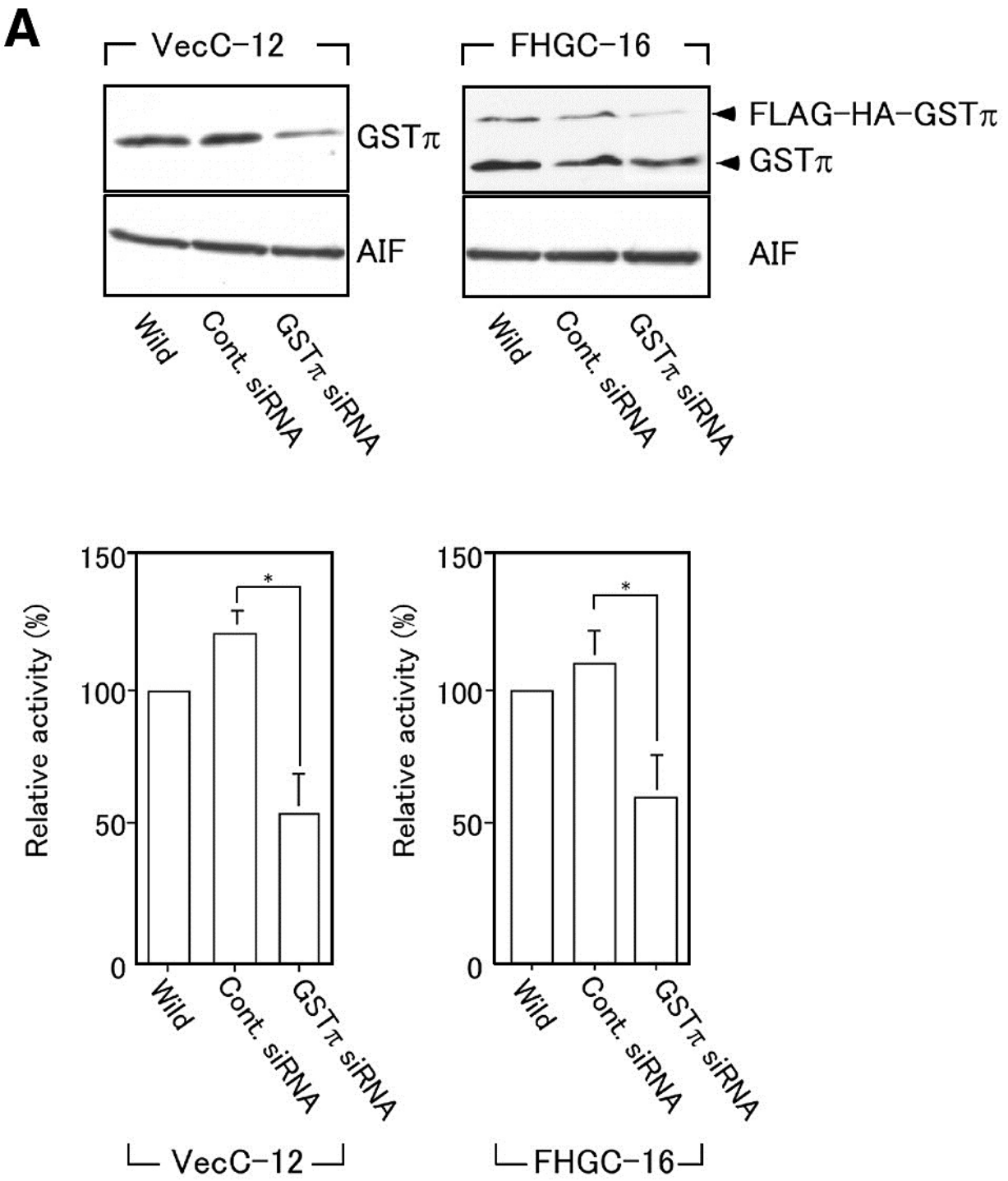
A
VecC-12
FHGC-16
GSTπ
AIF
FLAG-HA-GSTπ
GSTπ
Wild
Cont. siRNA
GSTπ siRNA
Relative activity (%)
150
100
50
0
*
VecC-12
FHGC-16

Figure 4.

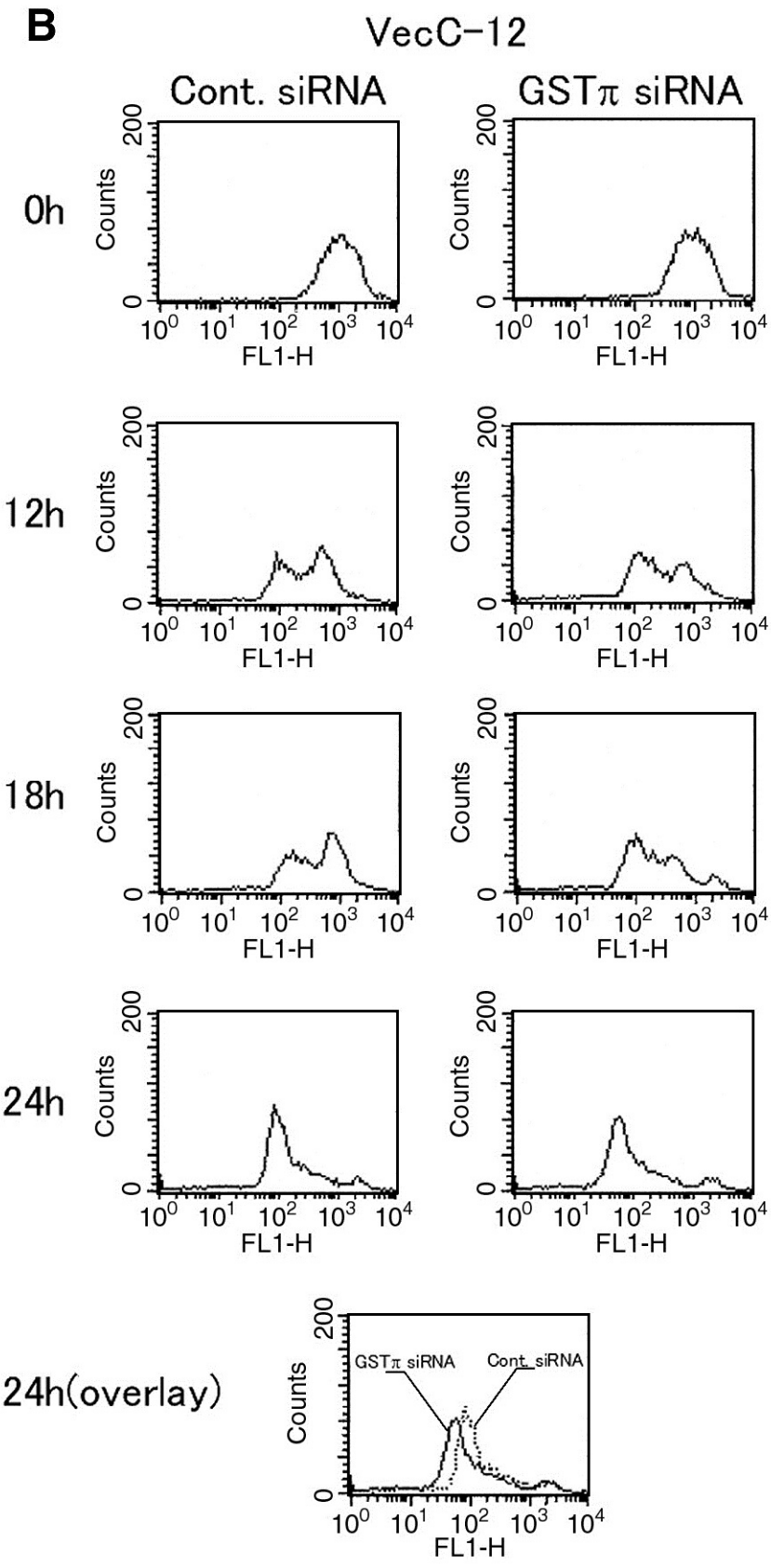
B
VecC-12
Cont. siRNA
GSTπ siRNA
0h
12h
18h
24h
24h(overlay)
Counts
FL1-H
GSTπ siRNA
Cont. siRNA

Figure 4.

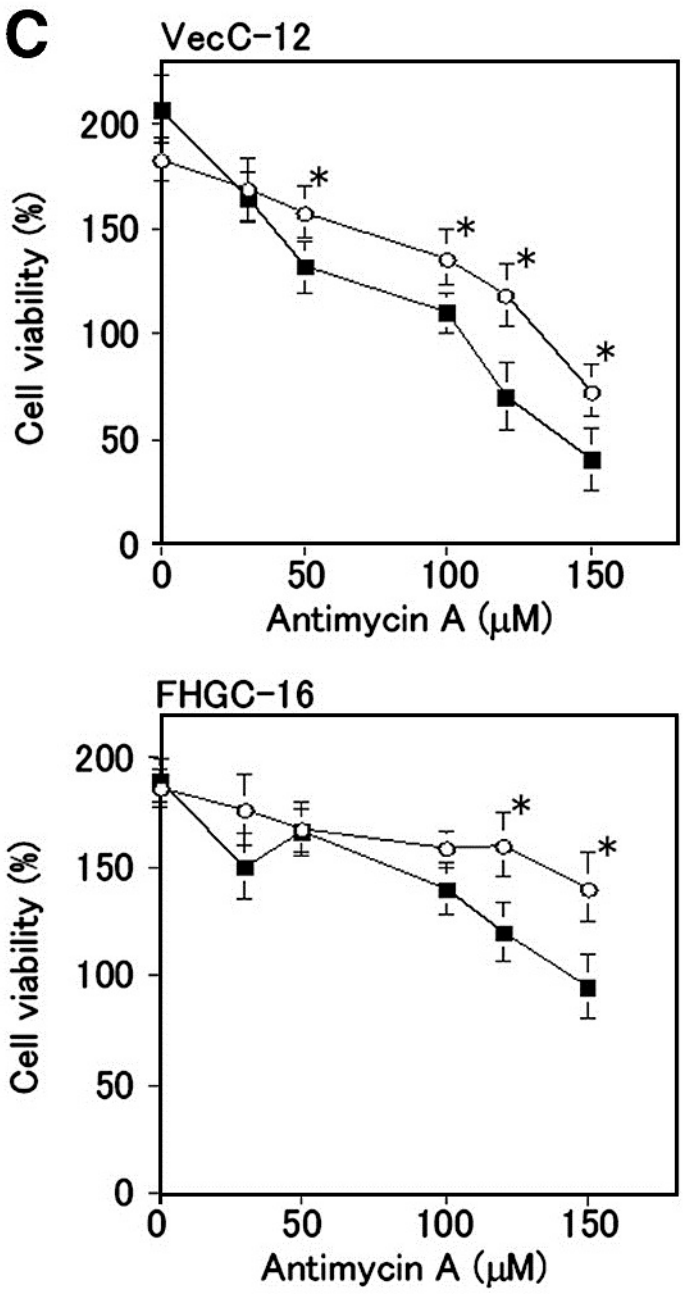
C
VecC-12
Cell viability (%)
200
150
100
50
0
0
50
100
150
Antimycin A (μM)
*
FHGC-16
Cell viability (%)
200
150
100
50
0
0
50
100
150
Antimycin A (μM)
*

Supplemental Figure 1.

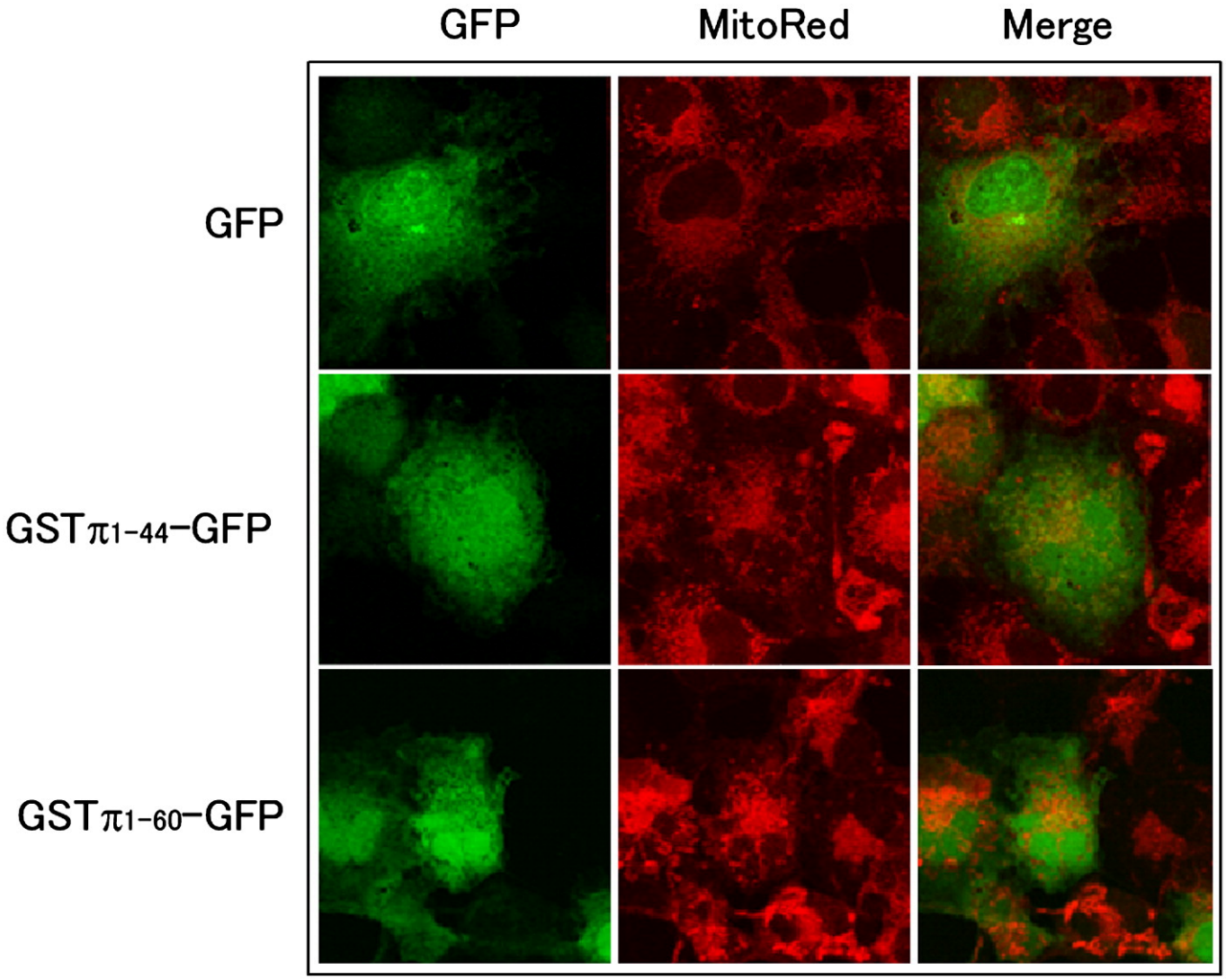

Supplemental Figure 2.

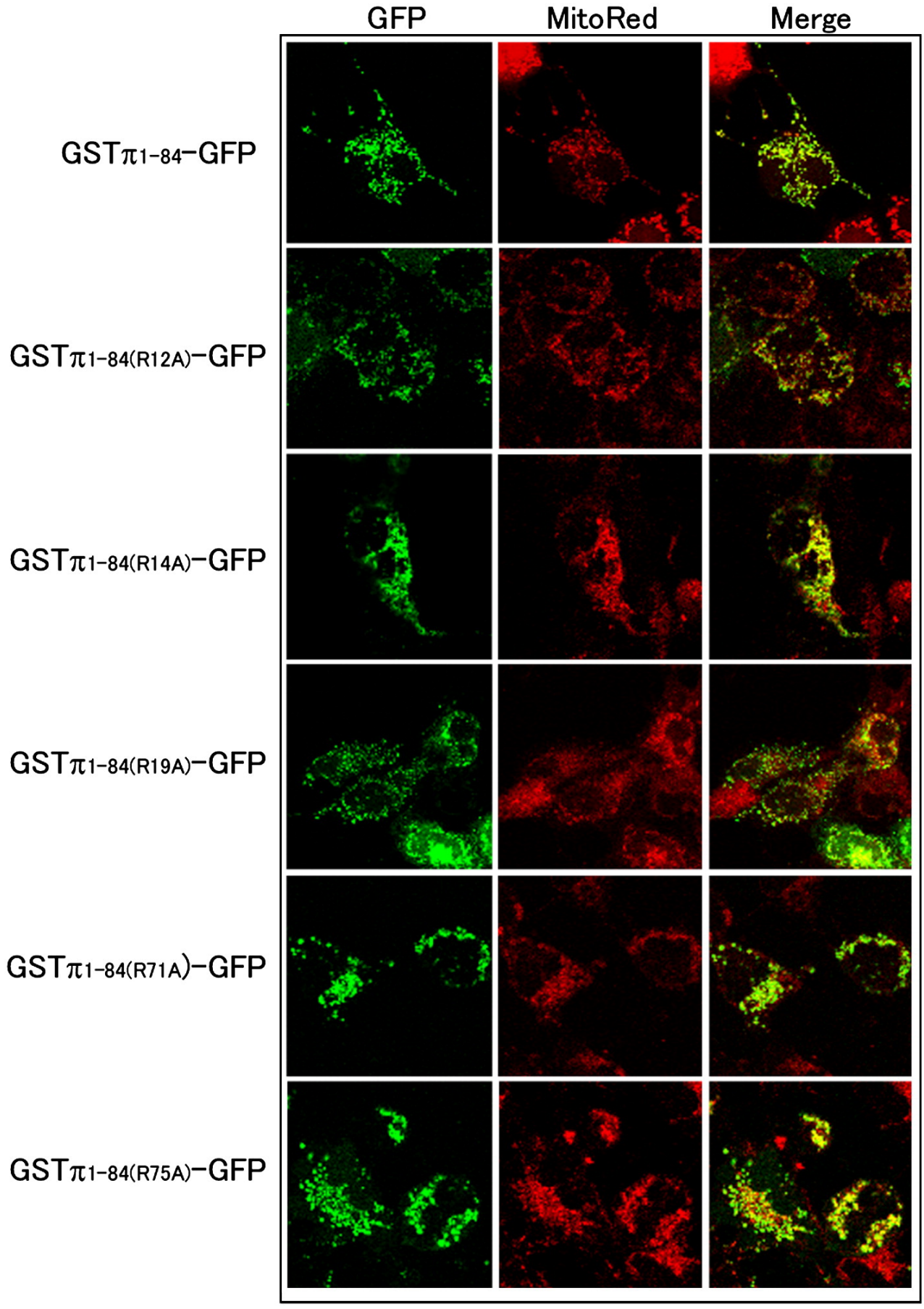

Supplemental Figure 3.

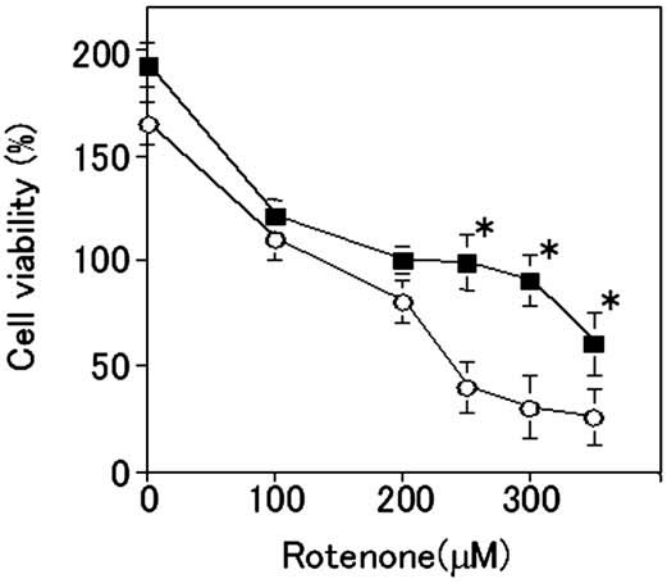

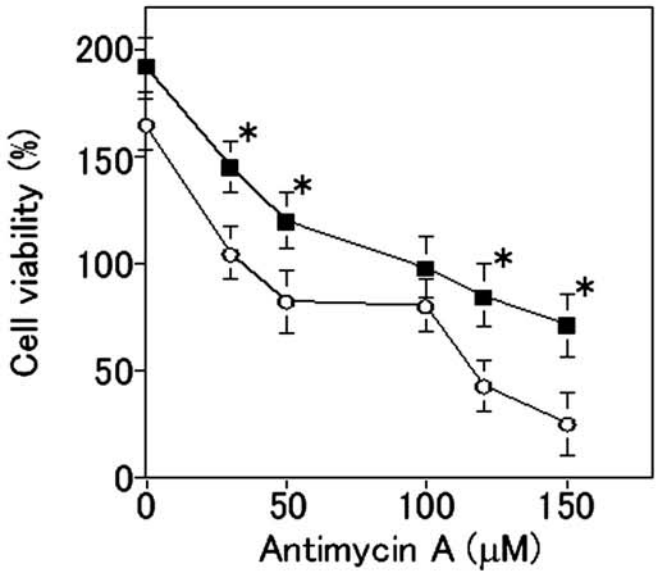

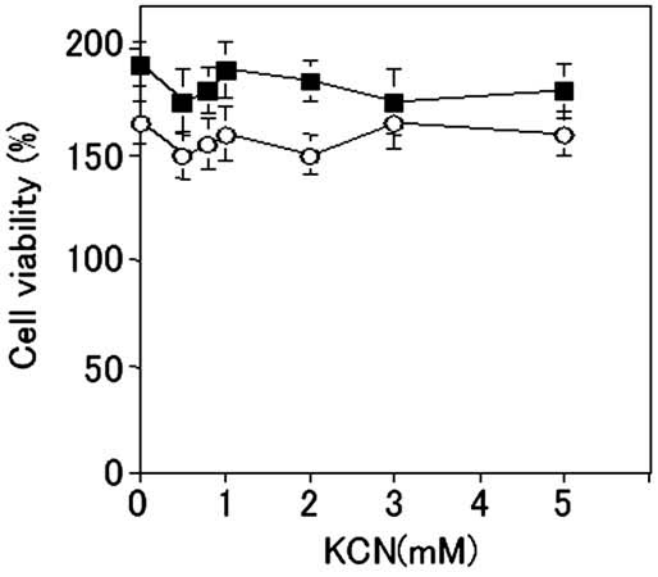

Supplemental Figure 4.